

University of Windsor

Scholarship at UWindor

Electronic Theses and Dissertations

Theses, Dissertations, and Major Papers

1-1-1968

Beta-gamma angular correlations and shape correction factor determinations in the decays of rhenium-186 and rhenium-188.

Murray L. Trudel
University of Windsor

Follow this and additional works at: <https://scholar.uwindsor.ca/etd>

Recommended Citation

Trudel, Murray L., "Beta-gamma angular correlations and shape correction factor determinations in the decays of rhenium-186 and rhenium-188." (1968). *Electronic Theses and Dissertations*. 6062.
<https://scholar.uwindsor.ca/etd/6062>

This online database contains the full-text of PhD dissertations and Masters' theses of University of Windsor students from 1954 forward. These documents are made available for personal study and research purposes only, in accordance with the Canadian Copyright Act and the Creative Commons license—CC BY-NC-ND (Attribution, Non-Commercial, No Derivative Works). Under this license, works must always be attributed to the copyright holder (original author), cannot be used for any commercial purposes, and may not be altered. Any other use would require the permission of the copyright holder. Students may inquire about withdrawing their dissertation and/or thesis from this database. For additional inquiries, please contact the repository administrator via email (scholarship@uwindsor.ca) or by telephone at 519-253-3000ext. 3208.

β - γ ANGULAR CORRELATIONS AND SHAPE CORRECTION FACTOR
DETERMINATIONS IN THE DECAYS OF Re^{186} AND Re^{188} .

by

Murray L. Trudel

A Thesis

Submitted to the Faculty of Graduate Studies through the Department
of Physics in Partial Fulfillment of the Requirements for
the Degree of Doctor of Philosophy at the
University of Windsor

Windsor, Ontario

1968

UMI Number: DC52628

INFORMATION TO USERS

The quality of this reproduction is dependent upon the quality of the copy submitted. Broken or indistinct print, colored or poor quality illustrations and photographs, print bleed-through, substandard margins, and improper alignment can adversely affect reproduction.

In the unlikely event that the author did not send a complete manuscript and there are missing pages, these will be noted. Also, if unauthorized copyright material had to be removed, a note will indicate the deletion.

UMI[®]

UMI Microform DC52628

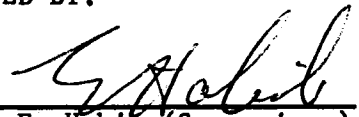
Copyright 2008 by ProQuest LLC.

All rights reserved. This microform edition is protected against unauthorized copying under Title 17, United States Code.


ProQuest LLC
789 E. Eisenhower Parkway
PO Box 1346
Ann Arbor, MI 48106-1346

110 X 6365


APPROVED BY:



Dr. E. E. Habib (Supervisor)



Dr. H. Ogata



Dr. F. Holuj

217497

ABSTRACT

The directional correlation between the nonunique first forbidden 935-Kev beta group and the 137-Kev gamma transition in the decay of Re^{186} , and the directional correlation between the nonunique first forbidden 1980-Kev beta group and the 155-Kev gamma transition in the decay of Re^{188} , have been measured as a function of energy. The beta-gamma angular correlation coefficient A_2 is found to have the following energy (W) dependence:

Re^{186} :

W	A_2
1.60	0.043 ± 0.004
1.80	0.059 ± 0.004
2.00	0.079 ± 0.004
2.20	0.085 ± 0.004
2.40	0.098 ± 0.004
2.60	0.093 ± 0.006

Re¹⁸⁸ :

<u>W</u>	<u>A₂</u>
3.01	0.133 ± 0.005
3.22	0.151 ± 0.004
3.42	0.161 ± 0.006
3.61	0.176 ± 0.004
3.81	0.183 ± 0.006
4.01	0.201 ± 0.004
4.21	0.216 ± 0.006

An investigation of the possible existence of a perturbation of the angular correlation caused by extranuclear fields has been carried out. No perturbation effect due to a magnetic hyperfine structure interaction or to an electric quadrupole interaction has been detected.

The shapes of the spectra of the 935-Kev and the 1980-Kev beta groups in the decays of Re¹⁸⁶ and Re¹⁸⁸ respectively have been investigated using the beta - gamma coincidence technique. It is found that these beta groups have the statistical shape: the shape correction factor C(W) for the 935-Kev beta transition is constant to within ±1%, and C(W) for the 1980-Kev beta transition is constant to within ±1.5%.

A search for the nuclear matrix element parameters Y, x and u

which are compatible with the experimental results was conducted.

The analysis was based upon the theoretical expressions of Kotani (1).

ACKNOWLEDGMENTS

I should like to thank Dr. E. E. Habib, under whose supervision this project was carried out, for his guidance and assistance. I should like also to thank Dr. H. Ogata who performed the calculations to determine the nuclear matrix element parameters.

Acknowledgments are due to Mr. W. Grewe for constructing the decoupling lens.

Finally, I am indebted to the NRC for its financial support in the form of Graduate Fellowships.

TABLE OF CONTENTS

	Page
ABSTRACT	iii
ACKNOWLEDGMENTS	vi
LIST OF TABLES	x
LIST OF FIGURES	xi
CHAPTER I. INTRODUCTION	1
CHAPTER II. THEORY OF ANGULAR CORRELATIONS OF NUCLEAR RADIATIONS	4
A. Unperturbed Angular Correlations	4
a. Introduction	4
b. The importance of Angular Correlations	5
c. The Theoretical Directional Correlation Function $W(\theta)$	7
d. Beta-Gamma Angular Correlation	10
B. Perturbed Angular Correlations	11
a. Introduction	11
b. Static Quadrupole Interaction	13
c. Time-Dependent Magnetic Interaction	14
d. Magnetic Decoupling	15
CHAPTER III. THE THEORY OF NUCLEAR BETA DECAY	17
A. Introduction	17
B. Form of the Beta Interaction	18
C. The Kurie Plot	22

	Page
CHAPTER IV. DESCRIPTION OF THE APPARATUS	25
A. The Coincidence Spectrometer	25
B. The Coincidence Circuit	29
C. Geometrical Correction Factors	33
CHAPTER V. BETA-GAMMA DIRECTIONAL CORRELATIONS IN Re ¹⁸⁶ AND Re ¹⁸⁸	39
A. Introduction	39
B. Experimental Procedure	39
C. Treatment of Data	46
CHAPTER VI. MAGNETIC AND QUADRUPOLE INTERACTIONS IN Re ¹⁸⁶ AND Re ¹⁸⁸ ANGULAR CORRELATIONS	50
A. Introduction	50
B. Magnetic Decoupling Experiment	51
C. Electric Quadrupole Interaction	59
CHAPTER VII. SHAPE OF BETA SPECTRA IN THE DECAYS OF Re ¹⁸⁶ AND Re ¹⁸⁸	68
A. Introduction	68
B. Experimental Procedure	68
C. Treatment of Data	71
D. Results	71
CHAPTER VIII. DETERMINATION OF NUCLEAR MATRIX ELEMENT PARAMETERS IN THE FIRST-FORBIDDEN BETA DECAY OF Re ¹⁸⁶ AND Re ¹⁸⁸	75
A. Introduction	75
B. Theoretical Formulation	75
C. Method of Analysis	77
D. Re ¹⁸⁶ and Re ¹⁸⁸ Results	78

	Page
CHAPTER IX. CONCLUSION	82
BIBLIOGRAPHY	83
VITA AUCTORIS	85

LIST OF TABLES

	Page
I. Allowed and First-Forbidden Nuclear Matrix Elements and Their Selection Rules	23
II. The Variation in Resolving Time 2τ for a β - γ Directional Correlation Run in Re^{186}	45
III. The Values of the A_2 Coefficients Obtained for the β - γ Directional Correlation in Re^{188}	48
IV. The Values of the A_2 Coefficients Obtained for the β - γ Directional Correlation in Re^{186}	49
V. The Values of the A_2 Coefficient ($W = 2.0$) Obtained for the β - γ Directional Correlation in Re^{186} Utilizing the Magnetic Decoupling Lens	58
VI. Summary of Experimental Results Obtained from Time Spectra Analysis	66
VII. A Tabulation of End Point Energies for Re^{186} and Re^{188}	72
VIII. Comparison of Theoretical Predictions Based on the Parameter Set $Y = 4.45$; $u = 0.09$; $x = -0.40$ With Experimental Results for Re^{186}	79
IX. Comparison of Theoretical Predictions Based on the Parameter Set $Y = 2.74$; $u = 0.06$; $x = 0.085$ With Experimental Results for Re^{188}	81

LIST OF FIGURES

	Page
1. Schematic of a Directional Correlation Measurement	9
2. Schematic Diagram of the Electron-Gamma Directional Correlation Spectrometer	26
3. Triangular Field Distribution for the Gerholm Instrument	27
4. A Block Diagram of the Fast-Slow Coincidence Arrangement	30
5. The Fast Coincidence Circuit	32
6. Discriminator Voltage Curve	34
7. Resolution Curve	34
8. The P_0 and P_2 Baffles	37
9. Principal Branches of Decay Scheme of Re^{186}	40
10. Principal Branches of Decay Scheme of Re^{188}	41
11. Low Energy Gamma Pulse Height Distribution from Re^{188}	44
12. Low Energy Gamma Pulse Height Distribution from Re^{186}	44
13. Schematic of the Decoupling Lens and of the Experimental Arrangement Used in the Magnetic Decoupling Experiment	52
14. Plot of Current vs Magnetic Field for the Decoupling Lens	54
15. Profiles of the 624-Kev Ba^{137} Electron Conversion Line for 0-KG and 3-KG Fields in the Decoupling Lens	55
16. A Time Spectrum	61
17. Experimental Arrangement for Time Spectra Analysis	62
18. Time Spectrum for the β - γ Cascade in Re^{186} Accumulated in the 90° Position (Run No. 1)	64

	Page
19. Pulse Height Distribution for the Beta Particles Focussed on the Plastic Scintillator in the Beta Spectrometer	70
20. Fermi Plot of the Inner Beta Spectrum of Re ¹⁸⁶	73
21. Fermi Plot of the Inner Beta Spectrum of Re ¹⁸⁸	74

CHAPTER I

INTRODUCTION

The angular correlation between successive nuclear transitions is frequently used to determine nuclear characteristics, such as the multipolarities, characters and mixing ratios of the transitions as well as the spins and parities of the levels involved. Provided the experimentally obtained angular correlation represents the true unperturbed relative directional distribution pattern one can infer the relevant nuclear parameters in a straightforward way from the theory of angular correlations.

It is well known that extranuclear fields can cause strong perturbations of the angular correlation (2). The nuclear magnetic dipole moment couples to external magnetic fields and the nuclear quadrupole moment will cause a similar coupling to electric field gradients. In both cases the coupling results in a precession around the external field (gradient) axis. If the coupling is sufficiently strong the nuclei change their initial orientation resulting in a smearing out of the angular correlation. A knowledge of the magnitude of these effects is of importance for the interpretation of the experimental results.

The beta-gamma directional correlations for the (935-Kev beta) (137-Kev gamma) cascade in Re^{186} , and the (1980-Kev beta)(155-Kev gamma) cascade in Re^{188} have been previously measured by a number of authors. In particular, the (935-Kev beta)(137-Kev gamma) directional correlation

in Re^{186} has been determined with good statistical accuracy by Novey et al (3), and with poor statistical accuracy by Dulaney et al (4); the (1980-Kev beta)(155-Kev gamma) directional correlation in Re^{188} has been determined by Wyly et al (5) but with extremely poor statistical accuracy. It was assumed by these authors that their results represented the unattenuated directional correlation. However, no significant attempt was made to determine this point experimentally.

The present research concerns itself with the accurate determination of the true unperturbed directional correlations in Re^{186} and Re^{188} . A serious investigation of the possible existence of perturbation mechanisms was carried out.

In addition to the directional correlation studies that have been conducted, much research has been done to try to unravel the shapes of the nonunique first forbidden 935-Kev and 1980-Kev beta transitions in the decays of Re^{186} and Re^{188} respectively. Different results have been obtained by various authors.

Porter et al (6) examined the 935-Kev beta spectrum in coincidence with the 137-Kev gamma transition and found that the spectrum exhibits deviations from the allowed shape. The shape correction factor was found to increase by 18% from 150-Kev to 900-Kev. On the other hand Koerts (7) and Bashandy et al (8), utilizing the coincidence technique, have reported an allowed shape for the 935-Kev beta transition. However, they do not indicate the accuracy with which the shape of the beta spectrum was determined. Johns et al (9) have also reported an allowed shape for the 935-Kev beta transition but their method of analysis

involved subtracting out the 935-Kev beta spectrum from a composite beta spectrum, a method which is not nearly as sensitive to departures from the allowed shape as the coincidence technique.

Similar results have been obtained for the 1980-Kev beta transition in Re^{188} . According to Johns et al (9), the spectrum exhibits deviations from the allowed shape. However, the subtraction procedure employed in their analysis could seriously affect the shape of the beta distribution. Bashandy et al (8) have reported an allowed shape for the 1980-Kev beta transition, but they do not give the accuracy with which the shape of the beta spectrum was determined.

In the present investigation the shapes of the spectra of the 935-Kev and the 1980-Kev beta groups have been studied using the β - γ coincidence technique in order to determine accurately the shape correction factors $C(W)$ for these beta transitions. The values of $C(W)$ thus obtained can then be used in the determination of the nuclear matrix elements involved in the beta transitions.

It is hoped that the research reported in this thesis will contribute in a positive manner to the body of knowledge already accumulated on the decays of Re^{186} and Re^{188} .

CHAPTER II

THEORY OF ANGULAR CORRELATIONS OF NUCLEAR RADIATIONS

A. Unperturbed Angular Correlations

a. Introduction. The probability of emission of a particle or quantum by a radioactive nucleus depends in general on the angle between the nuclear spin axis and the direction of emission. Under ordinary circumstances, the radiation R emitted from a radioactive sample for the individual transition $I_a \xrightarrow{R} I_b$ will be isotropic in the laboratory coordinates because the nuclei are randomly oriented in space. If the transition $I_a \longrightarrow I_b$ is followed by a second transition $I_b \longrightarrow I_c$, the individual radiations from the second transition are likewise isotropic in the laboratory coordinates.

However, in a two step cascade transition, such as $I_a \xrightarrow{R_1} I_b \xrightarrow{R_2} I_c$ there is often an angular correlation between the directions of emission of two successive radiations R_1 and R_2 which are emitted from the same nucleus.

The existence of an angular correlation arises because the direction of the first radiation is related to the orientation of the angular momentum I_b of the intermediate level. This orientation can be expressed in terms of the magnetic - angular - momentum quantum number m_b with respect to some laboratory direction such as that of the first radiation. If I_b is not zero, and if the lifetime of the intermediate level is short enough so that the orientation of I_b persists, then the direction

of emission of the second radiation will be related to the direction I_b and hence to that of the first radiation.

An anisotropic radiation pattern can be observed only from an ensemble of nuclei that are not randomly oriented. One method of arriving at such an ensemble consists in picking out only those nuclei whose spins happen to lie in a preferred direction. This can be realized if the nuclei decay through successive emission of two radiations R_1 and R_2 . The observation of R_1 in a fixed direction k_1 selects an ensemble of nuclei that has a nonisotropic distribution of spin orientations. The succeeding radiation R_2 then shows a definite angular correlation with respect to k_1 .

In the following we use the term "angular correlation" as comprising "directional correlation" and "polarization correlation". In directional correlation only the directions of the two radiations are observed; in polarization correlation one determines also the linear or circular polarization of one or both of the radiations.

b. The Importance of Angular Correlations. A study of the angular correlation of radiations emitted or absorbed in nuclear processes has been one of the principal methods available for the nuclear spectroscopy of excited states.

The information that can be obtained from angular correlation work depends on the type of radiation observed (α , γ , β , e^-), on the properties that are singled out by the experiment (direction, polarization, energy), and on the extranuclear fields acting on the nucleus.

If we assume that the decaying nuclei are free, i.e., that no extranuclear fields act on the nucleus and disturb its orientation

in the intermediate state, then, to the extent that this can be realized in practice, angular correlation measurements provide information about the properties of the nuclear levels involved and about the angular momenta carried away by the radiations. To be more precise, the $\gamma - \gamma$ directional correlation yields the spins of the nuclear levels and the multipole orders of the gamma transitions. The gamma matrix elements which describe the transitions, and hence the directional correlation, provide no information on nuclear structure which would check the validity of nuclear models. The relative parities of the nuclear levels can be determined if one measures the directional correlation involving an $e^- - \gamma$ cascade. The $e^- - \gamma$ directional correlation depends in general on a combination of normal conversion matrix elements and gamma matrix elements. If in addition to the normal conversion matrix elements there appear penetration matrix elements then some information on nuclear structure can be derived (10). The directional correlation of a $\beta - \gamma$ cascade depends not only on the spins and parities of the nuclear levels and the multipole orders of the transitions but also depends very strongly on the matrix elements for the beta transition which in turn are dependent on the details of nuclear structure. A unique determination of the beta matrix elements could provide a test for a nuclear model which describes the states involved.

The information that can be obtained from the influence of extranuclear fields on the nuclear angular correlation is also multifold. Very often, one can determine the quadrupole coupling $Q \partial^2 V / \partial z^2$ (Q = quadrupole moment; $\partial^2 V / \partial z^2$ = electric field gradient) from the

change of the correlation due to extranuclear fields. In many cases, one can measure the g - factor of an excited nuclear state by observing the directional correlation as a function of an external magnetic field. From the g - factor one gets the magnetic moment if the spin of the nuclear state is known.

c. The Theoretical Directional Correlation Function $W(\theta)$.

The theory of angular correlation is highly developed and general expressions can be written down for even very complex situations. However, the general formulation of the theory is very complicated and is somewhat lengthy. Very good formulations of the theory are present in the literature (11). We will therefore present in this section a simple treatment of directional correlation theory that, while restricted in its usefulness, provides some insight into the correlation mechanism.

The common feature of all correlation problems is to be found in the fact that they involve an initial nuclear state of sharp angular momentum I_1 and parity, that undergoes successive transformations, either emitting or absorbing radiations through intermediate states of sharp angular momenta I_a, I_b, \dots and sharp parity, and terminating as a nucleus with sharp angular momentum I_2 and parity. The properties of the radiations, the observation or lack thereof of their directions of motion, polarization properties, the presence or absence of any perturbation of the intermediate nuclear states by external fields (magnetic (hfs) and possibly quadrupole interactions) condition the specific correlation discussed.

We consider here the directional correlation of two successive

radiations for the case of an unperturbed intermediate state. The schematic picture of a directional correlation measurement is shown in Fig. 1. A nuclear cascade involving states a , b , c with spins I_a , I_b , I_c occurs through the successive emission of particles R_1 and R_2 (It is assumed here that the spins and parities of the states a , b , c are well defined). We denote here with $W(\theta)d\Omega$ the relative probability that the radiation R_2 is emitted into the solid angle $d\Omega$ at an angle θ with respect to R_1 .

The most convenient form in which to express the correlation function $W(\theta)$ is:

$$W(\theta) = \sum_{k=0}^{k_{\max.}} A_k P_k(\cos \theta) \quad (1)$$

The functions P_k are Legendre polynomials. The coefficients A_k contain all the physical information.

At this point we introduce the following nomenclature for a double cascade involving pure multipole radiations, viz, $I_a (L_1) I_b (L_2) I_c$ where I_a , I_b and I_c denote the angular momenta of the first, intermediate and final nuclear levels, and L_1 and L_2 are the angular momenta of the two successive radiations.

Three general rules for the coefficients A_k hold for all types of particles:

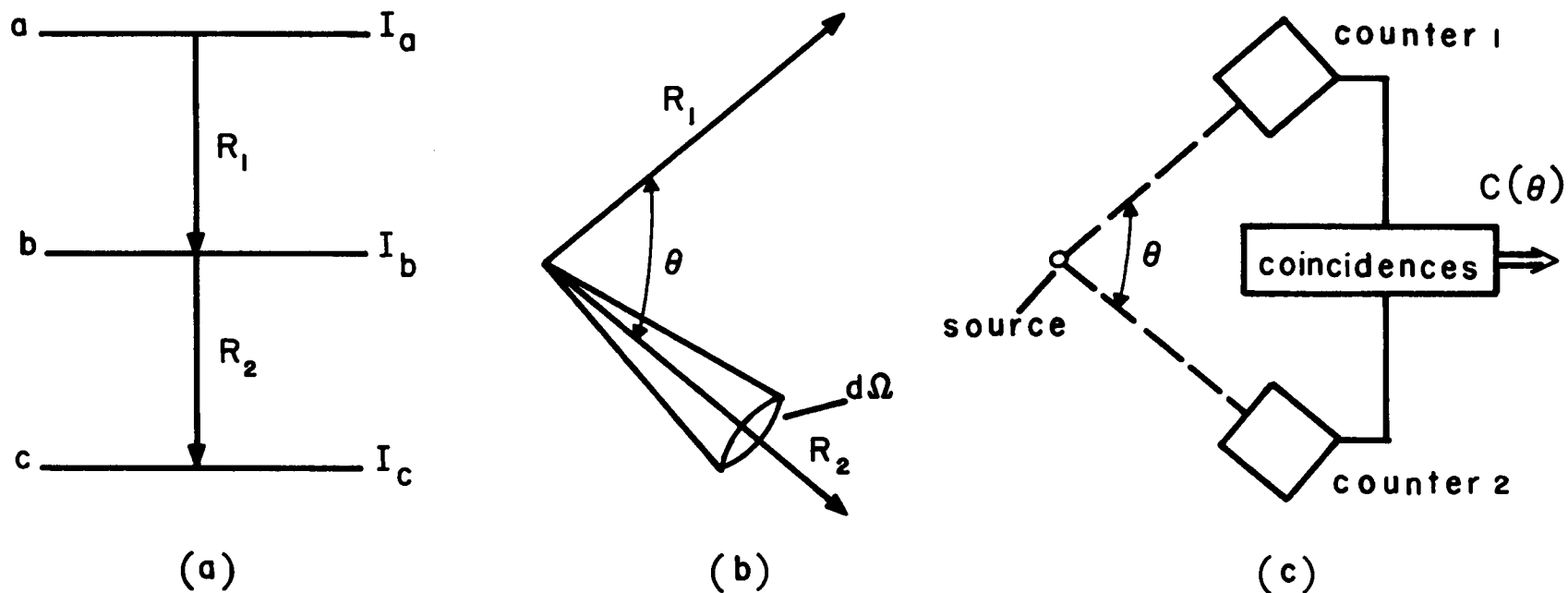


Fig. 1. Schematic of a Directional Correlation Measurement

(a) Nuclear cascade

(b) $W(\theta)d\Omega$ is the relative probability that the radiation R_2 is emitted into the solid angle $d\Omega$ at an angle θ with respect to R_1 .

(c) The two counters 1 and 2 subtend an angle θ at the source. From the coincidence count rate as a function of angle, $C(\theta)$, one obtains after suitable correction the correlation function $W(\theta)$.

$$k \text{ integer, even} \quad (1)$$

$$0 \leq k_{\max.} \leq \min. (2I_b, 2L_1, 2L_2) \quad (2)$$

$$A_k = A_k(a,b) A_k(b,c) \quad (3)$$

Rule 1 expressing the fact that only even Legendre polynomials appear, holds as long as one measures only directions and linear polarizations of the radiations. The observation of the circular polarization, however, introduces odd integers.

Rule 2 states that the highest term $k_{\max.}$ in the expansion is smaller than, or equal to, the smallest of the three numbers $2I_b$, $2L_1$, $2L_2$ where L_1 and L_2 are the angular momenta carried away by R_1 and R_2 . This rule implies an isotropic correlation if the angular momentum of either of the radiations or of the intermediate state equals 0 or 1/2. In the event that the cascade involves mixed radiations, i.e., $L_1 \rightarrow L_1 + L_1'$ and $L_2 \rightarrow L_2 + L_2'$, rule 2 becomes:

$$0 \leq k_{\max.} \leq \min. (2I_b, L_1 + L_1', L_2 + L_2')$$

Rule 3 expresses the fact that the coefficients A_k for a cascade can be broken up into two factors, each factor depending on only one transition of the cascade. The second factor $A_k(b,c)$, for instance, is entirely determined by the properties of the levels b and c and of the radiation R_2 . Numerical values for the factors $A_k(a,b)$ for given properties of the levels (a) and (b) and of the radiation R have been calculated for most cases of interest (11).

d. Beta - Gamma Angular Correlation. In the first transition of a $\beta - \gamma$ cascade, an electron and a neutrino are emitted simultaneously.

Formally, this event is described by treating the process as if a neutrino (antineutrino) enters the nucleus and a negatron (positron) is emitted. In a $\beta - \gamma$ correlation experiment one measures the direction of the electron while the neutrino escapes unobserved. The theoretical calculation of the angular correlation thus necessitates an averaging over all neutrino directions and over the spins of neutrino and electron.

The experimental technique of determining $\beta - \gamma$ directional correlations is quite straightforward. The fact, however, that the $\beta - \gamma$ directional correlation is a continuous and smooth function of energy makes precise measurements difficult. Since the energy dependence of A_2 provides the most useful information on the beta transition, the $\beta - \gamma$ directional correlation should be determined within as wide an energy range as possible.

The $\beta - \gamma$ directional correlation involving a first-forbidden beta transition is of the form:

$$W_{\beta-\gamma}(\theta) = 1 + A_2(E)P_2(\cos \theta) \quad (2)$$

where E = beta energy.

B. Perturbed Angular Correlations.

a. Introduction. The theory of the correlation of the directions of emission of a sequence of two particles by radioactive nuclei has been treated extensively in the literature. The conclusions of these treatments, however, are only applicable if the intermediate state of the nucleus, between the first and second emissions, is completely unperturbed.

The theory of extranuclear perturbations on angular correlations has been developed during the past 20 years to a high degree of completeness. A thorough treatment of the magnetic dipole and the electric quadrupole interactions, including time-dependent effects has been presented by Abragam and Pound (12). A comprehensive review of the theory of perturbed angular correlations has been presented by Karlsson et al (2).

The angular correlation of a cascade $I_i \rightarrow I \rightarrow I_f$ will, in general be altered as soon as the nuclei in their intermediate level I are subject to torques, due to the interaction of either the magnetic dipole moment μ with an extranuclear magnetic field B , or of the electric quadrupole moment Q with electric field gradients $\partial^2 V / \partial z^2$. In the semiclassical picture, these interactions produce a precession of the nuclei around the symmetry axis. The changing nuclear orientation results in an altered angular correlation. In quantum mechanical language, if the quantization axis is chosen to coincide with the direction of the first radiation, the interactions cause transitions among the m - substates. The second radiation is emitted from a level with an altered population distribution and this change is responsible for the attenuation of the correlation.

The semiclassical picture of a precessing nucleus adequately describes the situation if the extranuclear fields are static. However, there also exist time-dependent fields which produce a change in the correlation function. In this case, realized for example in certain viscous fluids, the fluctuating electric field gradients at the site of the nucleus induce transitions among the m - substates.

A major difference is exhibited between static and time-dependent interactions in polycrystalline sources. In the case of a static interaction, the angular correlation in a polycrystalline source is never wiped out completely because a certain fraction of nuclei experience the static field in such a direction that their correlation is unperturbed or only slightly attenuated. Static interactions in polycrystalline sources thus never reduce the correlation below a "hard core" value, the limit of maximum attenuation. Time-dependent interactions, however, can wipe out the correlation completely. This is due to the fact that the direction of the field at each nucleus changes continuously in a random manner. No quantization axis exists for which the populations of the m - substates remain constant. Eventually, all m - substates are equally populated for any choice of the quantization axis and the directional correlation is isotropic.

It is clear that the perturbation depends primarily on the magnitude and type of the interaction, and on the length of time it can act, i.e., on the mean life τ of the intermediate level. A knowledge of the magnitude of these effects is of importance for the interpretation of the experimental results.

b. Static Quadrupole Interaction. In most crystals strongly inhomogeneous fields are known to be present. Therefore one should quite generally expect an internal static quadrupole interaction to take place in solid sources. To what extent this will result in an attenuation of the angular correlation depends on the lifetime of the intermediate level and on the strength of the coupling.

Abragam and Pound (12) have derived the following expression for an angular correlation perturbed by a static interaction:

$$W(\theta) = \sum_k G_k A_k P_k(\cos \theta) \quad (3)$$

where the A_k are the coefficients of the expansion in Legendre polynomials of the unperturbed correlation. The G_k are attenuation coefficients which contain all the information on the perturbation of the angular correlation and depend only on the intermediate nuclear state and not on the radiative transitions to and from it.

c. Time-Dependent Magnetic Interaction. The escape of a beta particle from an atom takes place in a time that is short compared to the orbital period of the shell electrons. The sudden change in nuclear charge from Z to $Z \pm 1$ introduces a sudden perturbation into the electrostatic potential in which the shell electrons move. This sudden perturbation may cause excitations and ionization of the electron shell. Holes are formed by the "shake-off" of electrons when the electron-core readjusts itself to the new atomic number. Thus there exists a non-vanishing probability that the daughter atom is in a highly ionized and excited state following beta emission by the parent atom.

The picture after beta emission and subsequent hole formation is as follows: A hole is created which moves very rapidly to the outermost shell. This movement occurs mainly through Auger effects and hence more holes are created that also move outward. Once these holes have reached the outermost shell, they can decay only slowly and hence can persist long enough to cause very strong perturbations of the

angular correlation. As a consequence of the after effects of hole formation in the electron core there might be a magnetic coupling between the nucleus and the magnetic field produced by the excited and ionized atomic core.

The final recovery depends on the availability of free electrons to fill up the holes in the outer shell and neutralize the ion. In a conducting material such as a metal, free electrons from the conduction band are readily available. If the radioactive nuclei are embedded in a metallic environment one should therefore expect the total recovery time to be too short compared to the precession period to allow for any attenuation, although such an attenuation cannot be ruled out absolutely. If the radioactive atoms are placed in an insulator, however, the atom might remain in its ionized and excited state for a longer period of time. As a consequence of the presence of incomplete electronic shells, the nucleus is exposed to a strong magnetic field, which may be of the order of $10^5 - 10^6$ G. The nuclear spin I will couple to the atomic spin J , i.e., a hyperfine structure interaction will occur. Under normal circumstances J is randomly orientated and will be subject to rapid fluctuations in time due to the filling up of the electronic shells. The net result might be an additional time-dependent attenuation of the angular correlation pattern, provided the hfs interaction lasts sufficiently long to cause a deorientation of the nuclear spin system.

d. Magnetic Decoupling. It should be possible to obtain a decoupling of I and J with the aid of an external magnetic field applied in the direction of emission of the beta particles (longitudinal

decoupling). If the interaction energy between the external magnetic field B and the magnetic moment μ_e of the electron core is larger than the hfs interaction, a decoupling will take place (13), i.e.,

$$\mu_e \cdot B > \mu_n \cdot B_J \quad (4)$$

where μ_n is the nuclear magnetic moment and B_J is the magnetic field at the nucleus caused by the excited electron core. The required strength of the external field then becomes $B > \mu_n \cdot B_J / \mu_e$. A field of a few thousand G should be quite sufficient to achieve complete decoupling in most cases of interest. When decoupling has been obtained I and J both precess around the axis of the external field which is chosen to coincide with the quantization axis in the angular correlation experiment. The precession of I around this axis will not give rise to any attenuations of the angular correlation pattern since the population of the nuclear m - substates remains unaffected. Transitions between atomic m -substates and changes in the atomic configuration during the neutralization process will not change the nuclear spin orientation. The decoupled system should give only a pure quadrupole interaction in both metallic and insulating source environment.

CHAPTER III

THE THEORY OF NUCLEAR BETA DECAY

A. Introduction.

In the last few years the study of the laws of beta decay has been the object of many experimental and theoretical investigations. As a consequence, the form of the nuclear beta decay interaction is now well established. We know that beta decay violates parity conservation completely, and can be written as a combination of the vector (V) and axial-vector (A) interactions.

The fact that parity is not conserved has enlarged the number of possible experiments on nuclear beta decay. This increase in the number of experimental possibilities, together with our knowledge of the interaction law, has given nuclear beta decay a new aspect: in many cases we can determine the matrix elements involved in the beta transition and these matrix elements can be applied to the study of nuclear structure.

In general terms the processes of beta decay are to be described as nuclear transitions between states of equal mass number in which certain light particles are emitted, absorbed or both. Negatron and positron beta decay can then be represented as the transformation of one nucleon in the nucleus, according to:



where β^- is the ordinary negative electron beta ray and β^+ is a positron beta ray. In a similar way, ν represents the neutrino and $\bar{\nu}$ is the Dirac antineutrino.

In a simple physical description of the beta process, it is possible to think of the beta process as somewhat analogous to photon emission and to introduce phenomenologically an interaction which is responsible for the beta emission. Here the electron-neutrino field plays a role similar to that of the electromagnetic field in photon processes. But one striking difference is the strengths of these two types of coupling. Allowed gamma processes have lifetimes of the order of less than 10^{-10} seconds whereas the fastest beta process of comparable energy has a lifetime of 10^{-2} seconds.

B. Form of the Beta Interaction.

The beta decay interaction H can be written as the sum of a scalar term H_β and a pseudoscalar term H'_β :

$$H = H_\beta + H'_\beta + \text{h.c.} \quad (7)$$

$$H_\beta = g(\psi_f^* O Q^+ \psi_i)(\psi_e^* O \psi_\nu) \quad (8)$$

$$H'_\beta = g(\psi_f^* O Q^+ \psi_i)(\psi_e^* O \gamma_5 \psi_\nu) \quad (9)$$

where g = coupling constant

γ_5 = Dirac matrix

h.c. = Hermitean conjugate

In equations (8) and (9) O is an operator which in the first scalar product operates on the nuclear variables and in the second scalar product acts only in the space of the lepton variables. In equation (9)

however, the operator $O\gamma_5$ rather than O acts on the lepton variables. Ψ_f and Ψ_i represent the final and initial nuclear states whereas Ψ_e and Ψ_ν represent the electron and neutrino states. Q^+ is an operator which changes a neutron into a proton (β^- decay) but leaves its wave function otherwise unchanged. The operator Q^- (contained in the h.c. term) induces the reverse transition (β^+ decay). The lepton scalar product is to be evaluated at the position of the decaying nucleon and hence in equations (8) and (9) a sum over nucleons is implied. The O operators can be any operators which preserve relativistic invariance. For the beta decay interaction there are only 5 such operators:

- (a) $O =$ Scalar (S)
- (b) $O =$ Vector (V)
- (c) $O =$ Tensor (T)
- (d) $O =$ Axial-Vector (A)
- (e) $O =$ Pseudoscalar (P) (10)

If there is no way of choosing the appropriate form a priori, we must admit all five interactions and write:

$$H = H_\beta + H'_\beta + \text{h.c.} \\ = g \left[\sum_X C_X H_\beta(X) + \sum_X C'_X H'_\beta(X) + \text{h.c.} \right] \quad (11)$$

where $H_\beta(X)$ and $H'_\beta(X)$ refer to the forms of H_β and H'_β [equations (8) and (9)] obtained by the five choices in (10), and X stands for S, V, T, A and P. The C_X and C'_X are complex coupling constants. There are therefore 20 coupling parameters to be determined for the beta decay interaction, viz, the real and imaginary parts of the 10 coupling constants C_X and C'_X . Unless one measures some pseudoscalar quantity,

the use of $(H_\beta + H'_\beta)$ is an unnecessary complication and the same results follow from the use of H_β or H'_β . We consider only H_β in the following since it suffices for present purposes.

Fortunately, a simplification of the beta decay interaction H_β is in order. The discovery of parity non-conservation and the experimental results connected with this discovery have shown that only the vector (V) and axial-vector (A) interactions are present in the beta decay interaction. The Hamiltonian density H_β may then be written:

$$H_\beta = g[C_V H(V) + C_A H(A)] \quad (12)$$

where C_A and C_V are the axial-vector and vector coupling constants respectively.

Given the interaction, the decay probability of an electron with energy E per unit time is given by the well known quantum mechanical expression:

$$N(E)dE = (2\pi/\hbar)(H_{fi})^2(dN_F/dE_0) \quad (13)$$

where dN_F/dE_0 is the density of final states available to the system per unit range of total energy, and H_{fi} is the matrix element of the beta interaction between the initial (i) and final (f) states.

The matrix element H_{fi} can be expanded in a rapidly convergent series of terms characterized by successive integral values for the angular momentum of the electron-neutrino field with respect to the emitting nucleus. The largest term represents the allowed transitions; the successively smaller terms represent the forbidden transitions. The selection rules follow from inspection of the character of each term.

The first term (zero-order term) in the expansion of H_{fi} gives

the transition probability for the so-called ALLOWED beta spectrum. Physically, this corresponds to the emission of the leptons with zero orbital angular momentum and no change in parity in the nuclear states. The selection rules for allowed radiation are divided into two groups: FERMI selection rules and GAMOW-TELLER (G.T.) selection rules. For the vector (FERMI) interaction the selection rules are:

$$\Delta I = I_f - I_i = 0 \quad ; \quad \pi_i \pi_f = +1$$

where I_i and π_i , and I_f and π_f refer respectively to the angular momentum and parity of the initial (i) and final (f) nuclear levels involved in the transition. For the axial-vector (G.T.) interaction, the selection rules are:

$$\Delta I = 0, \pm 1 \quad (0 \not\rightarrow 0) \quad ; \quad \pi_i \pi_f = +1$$

For the case of allowed transitions, the zero-order term of H_{fi} yields two "nuclear matrix elements": the Fermi matrix element f_1 and G.T. matrix element f_σ . In terms of these nuclear matrix elements, the transition probability becomes:

$$N(E) dE = \frac{2\pi g^2}{\hbar} [C_V^2 |f_1|^2 + C_A^2 |f_\sigma|^2] \frac{dN_f}{dE_0} \quad (14)$$

The second term in the expansion of H_{fi} (first order term) is much smaller than the first term, and its effects can only be observed if the allowed transition cannot take place. This term gives the transition probability for the so-called "FIRST-FORBIDDEN" transitions, the lowest order nonallowed kind in which the electron-neutrino pair carries an orbital angular momentum $1\hbar$. The selection rules for the first-forbidden transitions are:

$$\Delta I = 0, \pm 1 \quad (0 \not\rightarrow 0) \quad ; \quad \pi_i \pi_f = -1 \quad (\text{FERMI})$$

$$\Delta I = 0, \pm 1, \pm 2 \quad \begin{matrix} (0 \not\rightarrow 0) \\ (0 \not\leftarrow 1) \\ (\frac{1}{2} \not\rightarrow \frac{1}{2}) \end{matrix} \quad ; \quad \pi_i \pi_f = -1 \quad (\text{G.T.})$$

Whereas allowed transitions are governed by the two nuclear matrix elements f_1 and f_0 , first-forbidden decay is governed by six nuclear matrix elements. They are summarized in Table I together with their selection rules.

C. The Kurie Plot

In the theory of beta decay the probability $N(\eta)d\eta$ that a beta ray with momentum between η and $\eta + d\eta$ will be emitted in unit time can be written as:

$$N(\eta)d\eta = \text{Constant} \cdot C(W)\eta^2 F(Z,\eta)(W_0 - W)^2 d\eta \quad (15)$$

where: $W = m/m_0 = (E + m_0 c^2) / m_0 c^2$

E = Kinetic energy of beta particles

W_0 = Beta disintegration energy

$F(Z,\eta)$ = Coulomb Correction Factor

$C(W)$ = Shape Correction Factor

Equation (15) can be rewritten in the following form:

$$[N(\eta)/\eta^2 C(W) F(Z,\eta)]^{1/2} = \text{Constant} \cdot (W_0 - W) \quad (16)$$

Therefore a straight line results when the quantity $[N(\eta)/\eta^2 C(W) F(Z,\eta)]^{1/2}$ is plotted against a linear scale of beta ray energy W . Such graphs are called Kurie plots or Fermi plots. They are especially useful for revealing deviations from the theory and for obtaining the upper energy limit W_0 , as the extrapolated intercept of $[N(\eta)/\eta^2 C(W) F(Z,\eta)]^{1/2}$ on the

TABLE I

Allowed and First-Forbidden Nuclear Matrix Elements and Their Selection Rules (λ is the Total Angular Momentum of the Lepton Field:

$$\Delta I \equiv |I_i - I_f| \leq \lambda \leq I_i + I_f$$

Where I_i and I_f Stand for the Initial and Final Nuclear Spins in the Beta Decay).

	Matrix Element	λ	ΔI	$\pi_i \pi_f$
Allowed	C_V^{f1}	0	0	+1
	$C_A^{f\sigma}$	1	$0, \pm 1$ ($0 \rightarrow 0$)	+1
First Forbidden	$C_A^{fi\gamma_5}$	0	0	-1
	$C_A^{f\sigma \cdot r}$			
	$-C_V^{fi\alpha}$	1	$0, \pm 1$ ($0 \rightarrow 0$)	-1
	$-C_V^{fr}$			
	$C_A^{fi\sigma x r}$			
	$C_A^{fB_{ij}}$	2	$0, \pm 1, \pm 2$ ($0 \rightarrow 0$) ($0 \leftarrow 1$) ($1 \rightarrow 1$) $\frac{2}{2}$ $\frac{2}{2}$	-1

energy axis.

The shape correction factor for all allowed transitions is a constant. Although it is found that many first-forbidden spectra have the allowed shape ($C(W) = \text{constant}$), it may occur that, for certain first-forbidden transitions, $C(W)$ is an energy dependent quantity. If such is the case, a plot of $[N(\eta)/\eta^2 F(Z, \eta)]^{\frac{1}{2}}$ vs. energy W will not yield a straight line.

In general, the shape correction factor $C(W)$ and the angular correlation coefficient $A_k(W)$ in the $\beta - \gamma$ angular correlation function:

$$W_{\beta-\gamma}(\theta, W) = \sum_k A_k(W) P_k(\cos \theta)$$

are complicated functions of the individual nuclear matrix elements (1). In principle, a comparison of the experimentally determined functions $C(W)$ and $A_k(W)$ with the theoretically predicted functions $C'(W)$ and $A_k'(W)$ for various combinations of the nuclear matrix elements permits a unique determination of the matrix elements involved in the beta transition. In practice, however, a unique determination of the matrix elements is difficult to achieve due to the limitations imposed by experimental errors. At best, one can hope to estimate the values of the matrix elements within a certain range of values.

CHAPTER IV
DESCRIPTION OF THE APPARATUS

A. The Coincidence Spectrometer

The coincidence spectrometer used for the beta-gamma directional correlation measurements on Re^{186} and Re^{188} is due to T.R. Gerholm (14). A schematic of the electron-gamma directional correlation spectrometer is given in Fig. 2.

Magnetic momentum selection is provided in the electron channel which consists of an iron encapsuled long lens beta ray spectrometer with "triangular field focussing". The triangular field distribution is depicted in Fig. 3. Magnetic field measurements show that the source is in a field free region and that the strength of the magnetic field increases roughly linearly with increasing distance from the source when measured along the axis of symmetry. Theoretical as well as experimental studies of this field distribution show that it gives a favourably high luminosity (source area x transmission) which compensates for the small geometrical dimensions of the instrument. Fairly large sources (ϕ 5mm.) can be used without sacrifice in resolution (relative width at half - maximum) the latter being about 3% at a transmission (effective solid angle in percent of 4π) of about 1.8% for the arrangement utilized in our measurements.

For the electron optics a somewhat modified version of the Hubert ring focus baffle system is used. The envelope baffle consists

217497

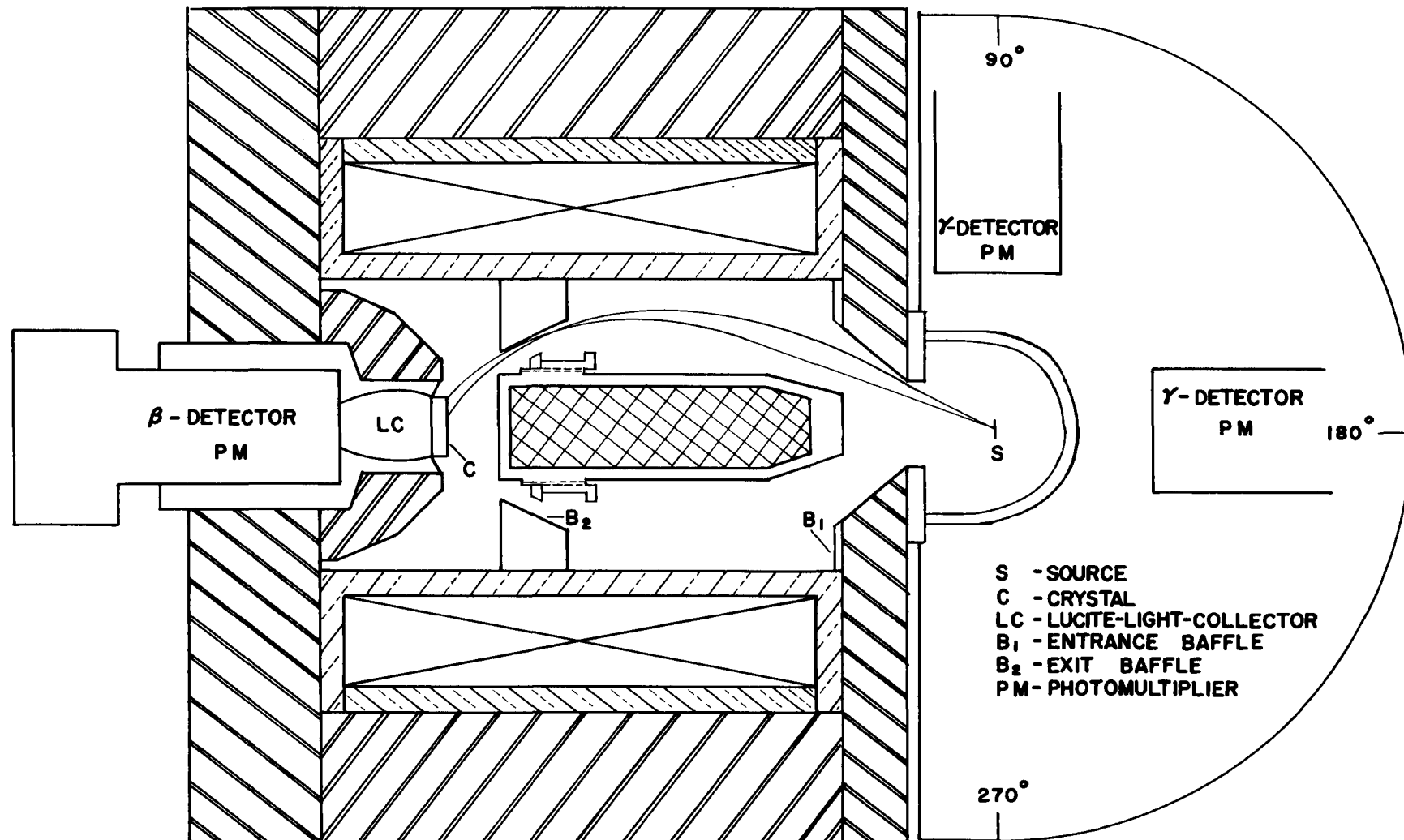


Fig. 2. Schematic diagram of the electron-gamma directional correlation spectrometer.

**FIELD STRENGTH
ARBITRARY UNITS**

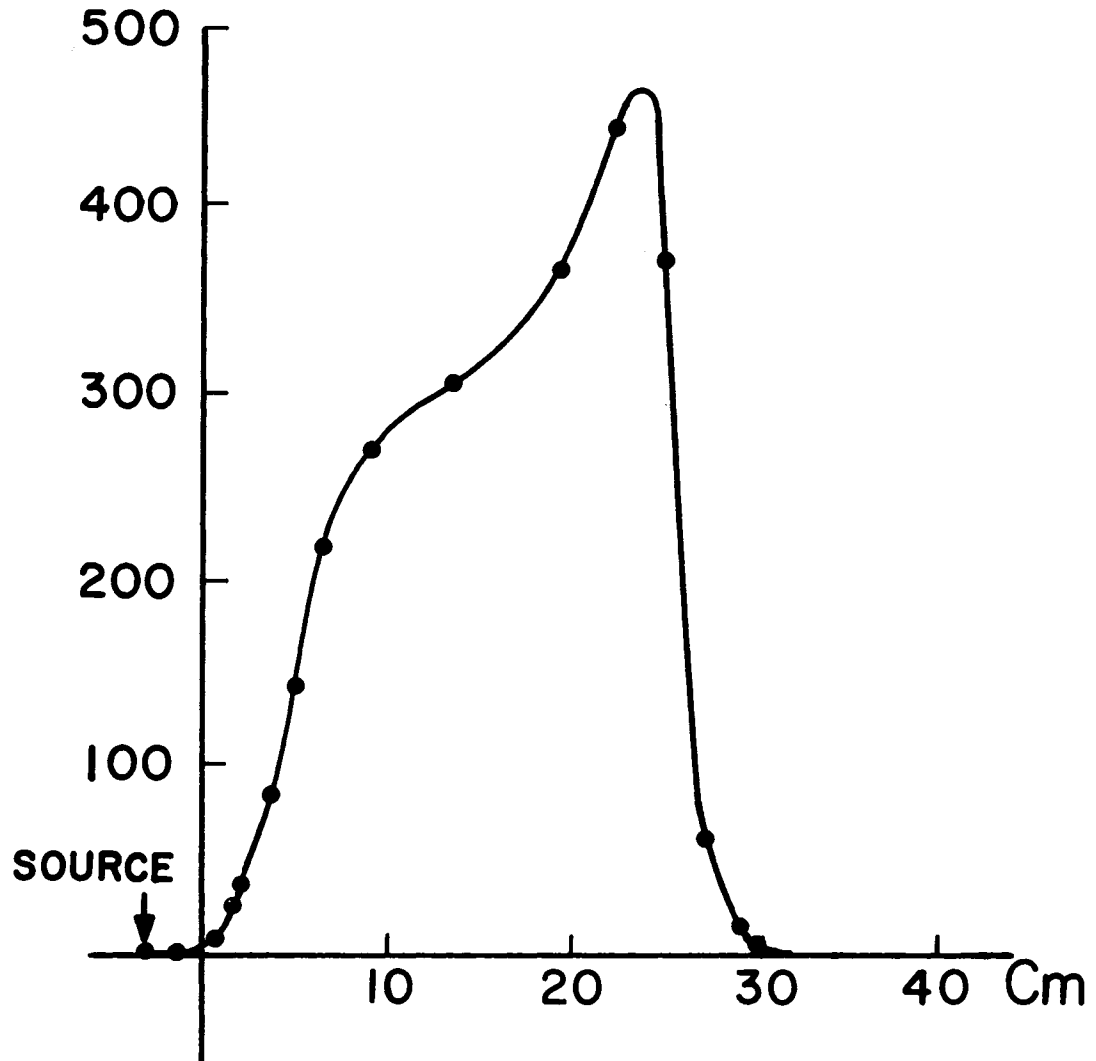


Fig. 3. Triangular field distribution for the Gerholm instrument as measured along the axis of symmetry.

of a cone and the internal baffle of an axially variable disc. As is shown in Fig. 2, this disc baffle defines the extreme rays. It therefore determines the mean angle of emission as well as the acceptance solid angle (transmission).

The beta detector consists of a plastic phosphor, in the shape of a disc, cemented onto a lucite light collector, of ellipsoidal shape, optically coupled to the central part of the photocathode of a 56-AVP photomultiplier tube. The scintillator is covered by a thin layer of MgO serving as a light reflector. The light collector acts as a light guide and renders it possible to obtain the required magnetic shielding.

The gamma detectors are provided with magnetic shielding through the use of Netic and Co-Netic wrapping materials. Each gamma detector consists of a NaI(Tl) scintillation crystal optically coupled to the photocathode of a 56-AVP photomultiplier tube. A $1\frac{3}{4}$ " x 2" crystal and a 2" x 2" crystal were utilized.

The gamma detectors are mounted at a fixed angle of 90° to one another on a movable arm which rests on the semicircular angular correlation table. The arm can be rotated through an angle of 90° about the source center. The physical arrangement is such that one detector (denoted the γ -1 probe) can be set at either the 270° or the 180° position, while the other detector (denoted the γ -2 probe) can be set at either the 180° or the 90° position. Rotation of the movable arm is accomplished via automatic probe positioning circuitry (15)

The sources used in the electron-gamma experiments are mounted

on thin aluminum rings. These rings are placed in a pedistal holder which slides against the source facing surface of the spectrometer iron flange.

Adjustments are provided for aligning the source with the symmetry axis of the baffle system and for aligning the center of rotation of the gamma detectors with the center of the source.

The vacuum system for the spectrometer is a very simple one. Operating pressures may be reached after five minutes of pumping.

B. The Coincidence Circuit

The coincidence circuit used for the beta-gamma correlation measurements is a slightly modified version of the "fast-slow" coincidence circuit due to Bell, Graham and Petch (16). The circuit was set up as shown in the block diagram of Fig. 4.

The outputs of the detectors are divided into a slow and a fast channel. The slow channel provides for pulse amplitude selection for each pulse train while the fast channel provides for time selection by performing the coincidence function on pulses unselected as to amplitude.

The detectors utilize high-gain 56-AVP photomultipliers. The gain of this tube when operated at 2000 volts is sufficient to ensure that the limiter (404-A pentode) will be cut off by the very first part of each pulse from the anode of the photomultiplier. The limited output pulses from the anode of the 404-A limiter are immediately shaped into very short pulses (≈ 10 nsec.) of height ≈ 0.5 volts and duration τ by means

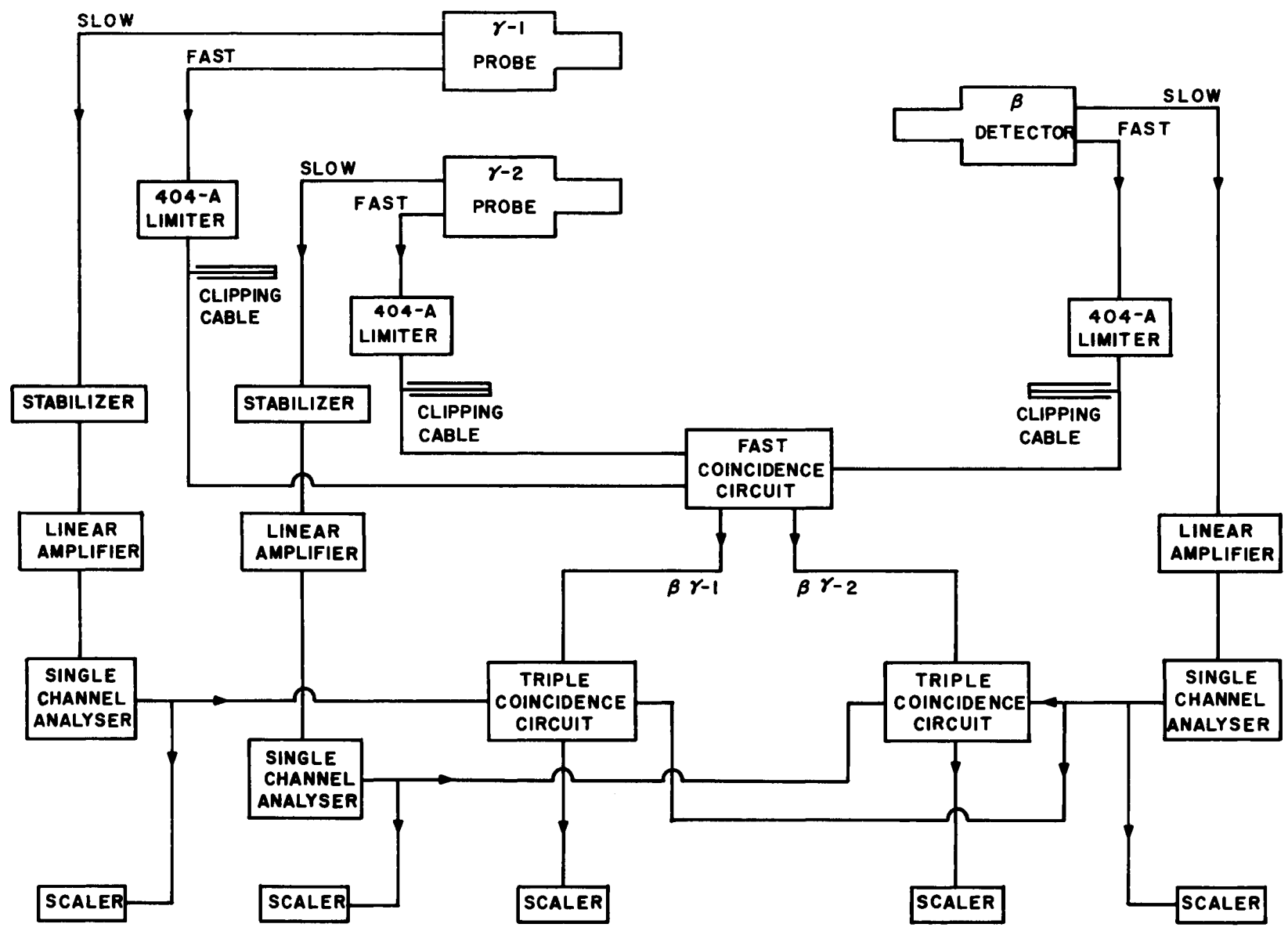


Fig. 4. A block diagram of the fast-slow coincidence arrangement.

of a short-circuited clipping cable with a transit time $\tau/2$. The width of these pulses essentially determines the resolving time 2τ of the fast coincidence circuit (Fig. 5). This circuit gives an output pulse for γ_1 - β and γ_2 - β coincidences only. The output from the fast coincidence circuit is fed to the slow triple coincidence circuit.

The slow pulses, which contain the pulse height information, are taken from a dynode near the anode of the photomultiplier. The gamma pulses are routed through a "spectrum stabilizer" (17) which "locks-on" the photopeak and thus provides for drift-free measurements. These pulses are then amplified, passed through a single channel analyser, and fed to the triple coincidence circuit and to a scaler. The slow beta pulse train is treated in an identical manner with the exception that it is not routed through the stabilizer.

The output from the triple coincidence circuit is fed to a scaler. The outputs from all the scalers are fed simultaneously to a Victor Printer (Model 12-10-321) and to a Tally Tape Perforator (Type 420).

The process of setting up the circuit for an experiment involves the following steps. First, each spectrometer is set on the position of the spectrum to be investigated. With the cables in the fast channels adjusted to approximate values, a discriminator voltage curve Fig. 6, is taken. This curve consists of a plot of the triples count rate versus discriminator voltage (Fig. 5). The discriminator voltage operating point is chosen in the center of the plateau thus assuring that the fast coincidence circuit produces an output for coincidence pulses only. The shape of this curve is quite insensitive to the energy of the

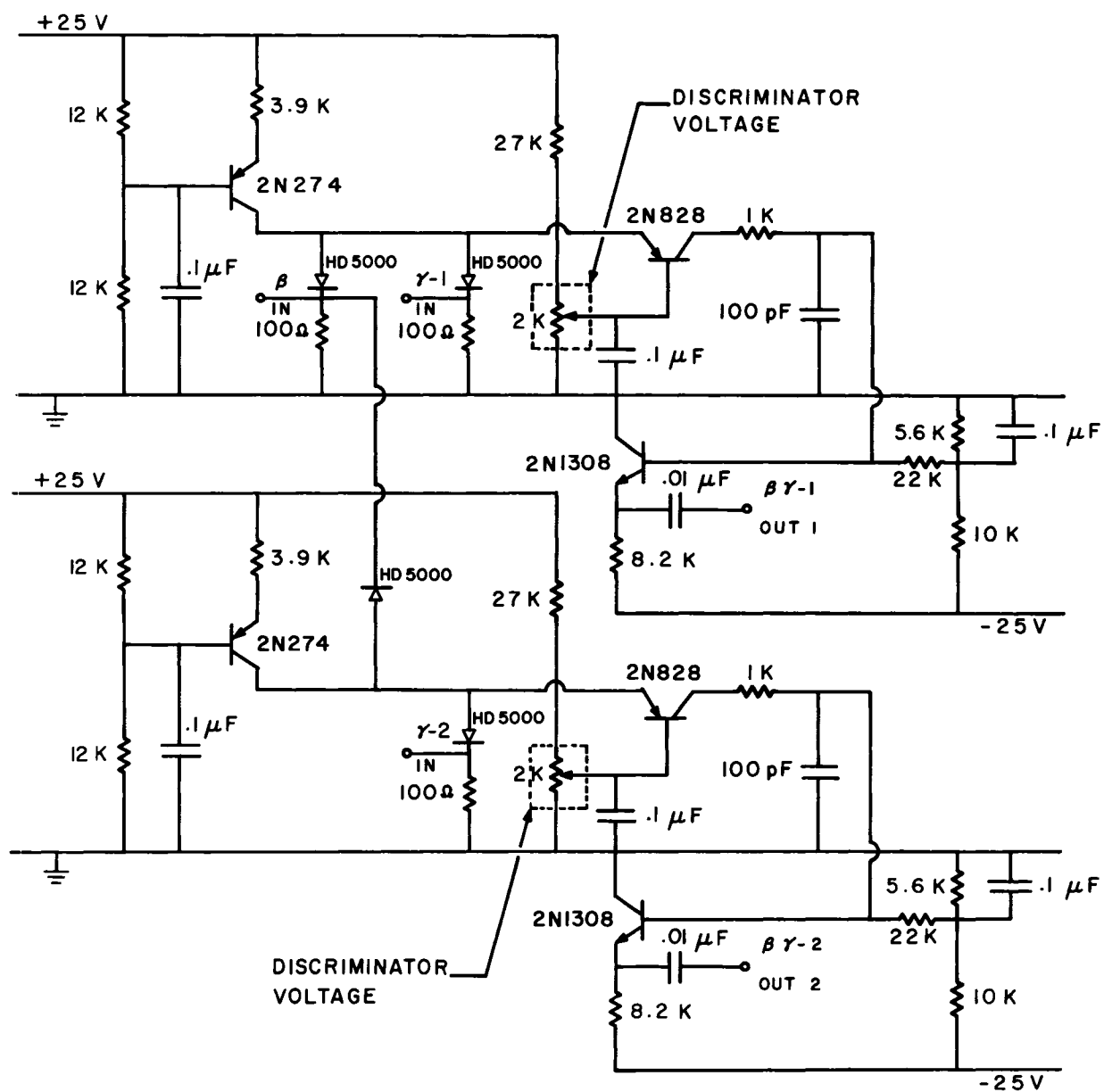


Fig. 5. The fast coincidence circuit.

radiations which produce the coincidences and therefore this setting need not be changed throughout an experiment. With the discriminator voltage properly set, a resolution curve such as Fig. 7, is obtained by altering the lengths of the cables between the photomultipliers and the fast coincidence unit. In order to obtain 100% coincidence efficiency it is essential that the resolution curve have a flat top and that the operating point be chosen near the center of this region. The width of the resolution curve at half-maximum gives the approximate value of the resolving time 2τ of the coincidence circuit. An accurate determination of the resolving time is obtained from the relation:

$$2\tau = N_c / N_\beta N_\gamma \quad (17)$$

where N_β = beta singles rate

N_γ = gamma singles rate

and where N_c is the chance coincidence rate, obtained by interposing a long delay (≈ 100 nsec.) in the beta fast channel and observing the resulting coincidence rate. As a check on the constancy of 2τ over long periods of time, the chance rate N_c was monitored regularly in the course of each experiment. In the angular correlation experiments to be described in Chapter V and Chapter VI resolving times of 15 and 20 nsec. were used for the γ -1 and γ -2 probes respectively.

C. Geometrical Correction Factors

The finite solid angles subtended by the gamma and electron detectors result in a smearing out of the angular correlation. Consequently, the observed angular correlation function $W_{\text{exp.}}(\theta)$ differs

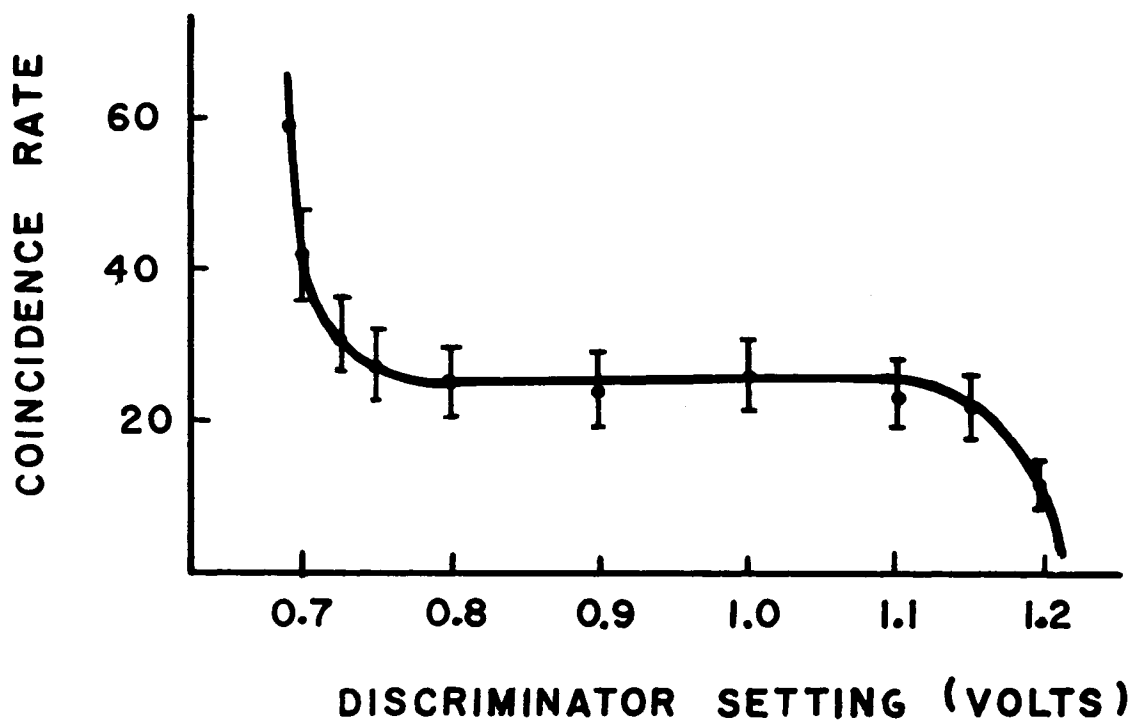


Fig. 6. Discriminator voltage curve.

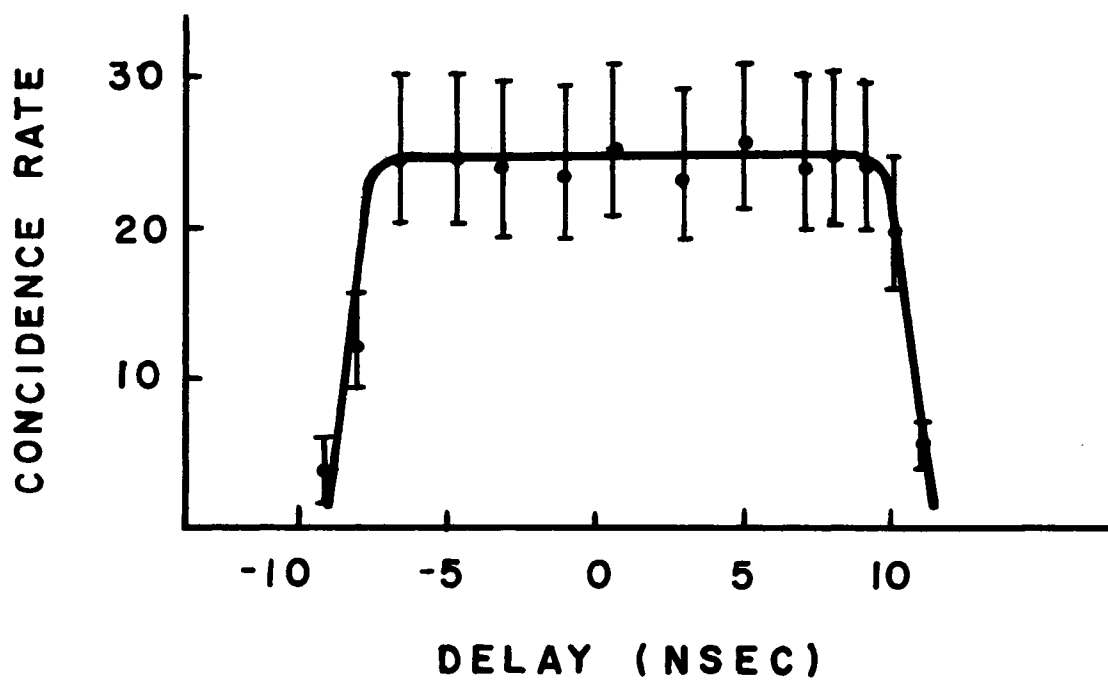


Fig. 7. Resolution curve.

slightly from $W(\theta)$ as given in equation (2) Chapter II. The experimentally measured directional correlation becomes:

$$W_{\text{exp.}}(\theta) = 1 + f_2 A_2 P_2(\cos\theta) \quad (18)$$

The factor f_2 is always less than unity and represents the smearing out of the angular correlation pattern due to the finite apertures in the two channels. This factor must be applied to the experimental results and should be known to better than 1%.

The correction factor f_2 may be written as a product:

$$f_2 = f_2(e^-) \cdot f_2(\gamma) < 1 \quad (19)$$

$f_2(\gamma)$ is the correction factor for the gamma channel and refers to either the "photopeak" correction factor or the "whole spectrum" correction factor, the choice of one or the other depending on the experimental procedure employed. These correction factors may be easily determined from published graphs (18) and tables (19). Under normal circumstances $f_2(\gamma)$ is fairly close to unity and therefore a minor error in this correction factor does not seriously affect the experimental results. For the directional correlation measurements described in this thesis the "photopeak" correction factor is required. However, at the low gamma energies of 137-Kev and 155-Kev in Re^{186} and Re^{188} respectively, the "photopeak" and "whole spectrum" correction factors are indistinguishable and hence, for convenience, the "whole spectrum" correction factors due to West (18) were utilized. For the directional correlations to be described in Chapter V, the values of $f_2(\gamma)$ obtained were:

$$\begin{aligned} f_2(\gamma) &= 0.957 && (\gamma\text{-2 Probe : 2" x 2" crystal}) \\ f_2(\gamma) &= 0.967 && (\gamma\text{-1 Probe : 1 3/4" x 2" crystal}) \end{aligned}$$

for both the 137-Kev and the 155-Kev gamma ray energies.

$f_2(e^-)$ is the correction factor for the electron channel. Its value is usually quite smaller than unity and cannot be easily determined with the required degree of accuracy by analytical methods. $f_2(e^-)$ must be determined experimentally. The appropriate expression for $f_2(e^-)$ is given (14) by:

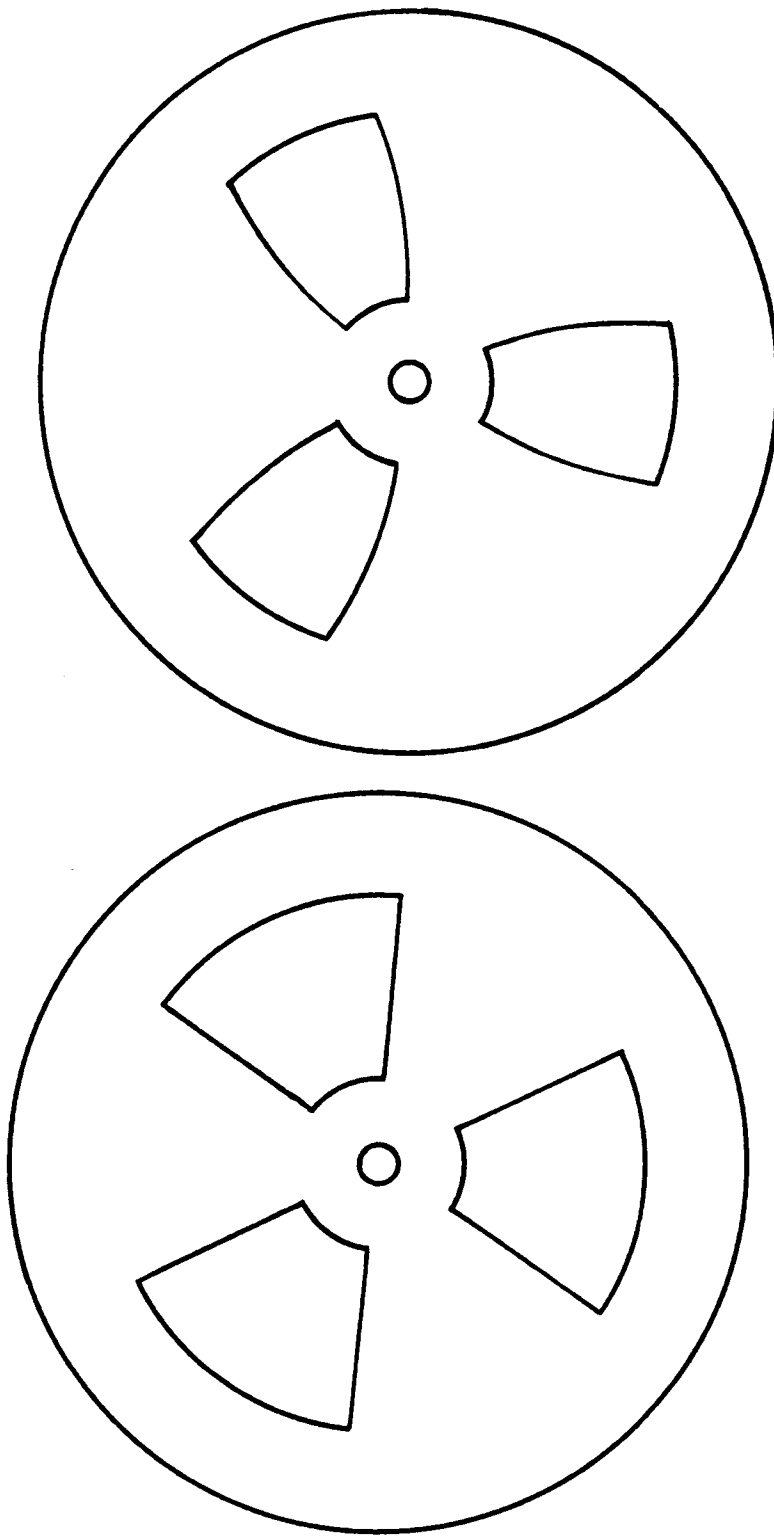
$$f_2(e^-) = \frac{\int_{\alpha_1}^{\alpha_2} \phi(\alpha) P_2(\cos \alpha) \sin \alpha d\alpha}{\int_{\alpha_1}^{\alpha_2} \phi(\alpha) \sin \alpha d\alpha} \quad (20)$$

where α_1 and α_2 represent the minimum and maximum electron take-off angles, $\phi(\alpha)$ is the electron detection efficiency at the angle α , and $P_2(\cos \alpha)$ is the usual Legendre polynomial. In order to determine $f_2(e^-)$ experimentally, the so-called P_0 and P_2 baffles, shown in Fig. 8, are used. The P_2 baffle has been made such that it simulates a P_2 distribution, whereas the P_0 baffle is used for normalization. The P_2 and P_0 baffles have openings cut in them each of which has an area given by:

$$a_2 = K \int_{\alpha_1}^{\alpha_2} P_2(\cos \alpha) \sin \alpha d\alpha \quad (21)$$

$$a_0 = K \int_{\alpha_1}^{\alpha_2} \sin \alpha d\alpha \quad (22)$$

respectively, where $K = \text{constant}$. The P_2 and P_0 baffles are inserted in turn in the frame of the entrance baffle in front of the source, perpendicular to the axis of the spectrometer, and pressed against the inner surface of the source facing iron flange. The counting rates



P₀ BAFFLE P₂ BAFFLE

Fig. 8. The P₀ and P₂ Baffles.

obtained are $N(P_2)$ and $N(P_0)$ respectively, and are proportional to the areas of the baffle openings, i.e.:

$$\frac{N(P_2)}{N(P_0)} = \frac{\int_{\alpha_1}^{\alpha_2} \phi(\alpha) P_2(\cos \alpha) \sin \alpha d\alpha}{\int_{\alpha_1}^{\alpha_2} \phi(\alpha) \sin \alpha d\alpha} = f_2(e^-) \quad (23)$$

Since $N(P_2)$ and $N(P_0)$ are single counting rates they can be easily determined with the required statistical accuracy. A complete description of the P_0 and P_2 baffles and of the procedure to be employed in the determination of $f_2(e^-)$ is given by Gerholm (14).

For the directional correlations to be described in Chapter V, the value of $f_2(e^-)$ obtained was:

$$f_2(e^-) = 0.725 \pm 0.003$$

CHAPTER V

BETA GAMMA DIRECTIONAL CORRELATIONS IN Re^{186} AND Re^{188}

A. Introduction

The decay scheme of Re^{186} is shown in Fig. 9 (20). The directional correlation between the nonunique first forbidden 935-Kev beta group and the 137-Kev gamma transition has been measured as a function of beta energy above 300-Kev. The lifetime of the lower 2^+ state in Os^{186} is 0.8 nsec.

The decay scheme of Re^{188} is shown in Fig. 10 (20). The directional correlation between the nonunique first forbidden 1980-Kev beta group and the 155-Kev gamma transition has been measured as a function of beta energy above 1-Mev. The lifetime of the lower 2^+ state in Os^{188} is 0.7 nsec.

For both of these transitions the spin sequence is $1^-(\beta)2^+(\gamma)0^+$. From the first forbidden character of the 935-Kev and 1980-Kev beta transitions a correlation function $W(\theta)$ of the form $[W(\theta) = 1 + A_2 P_2(\cos\theta)]$ is anticipated if contributions from the third and higher order forbidden terms are neglected.

B. Experimental Procedure

In order to check the performance of the electronics and to test the validity of the normalization and chance determination procedures, a measurement of the beta-gamma directional correlation in Co^{60} was made.

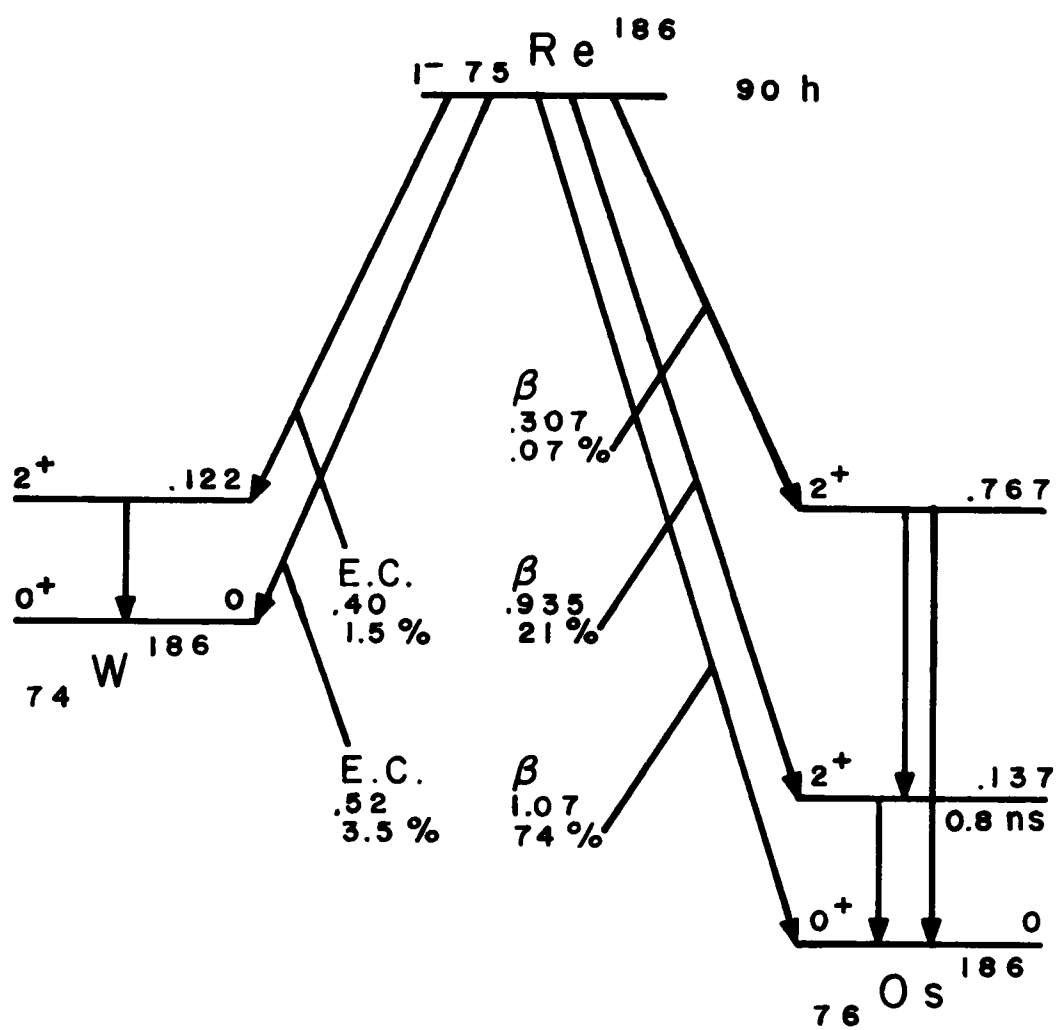


Fig. 9. Principal branches of decay scheme of Re^{186} .

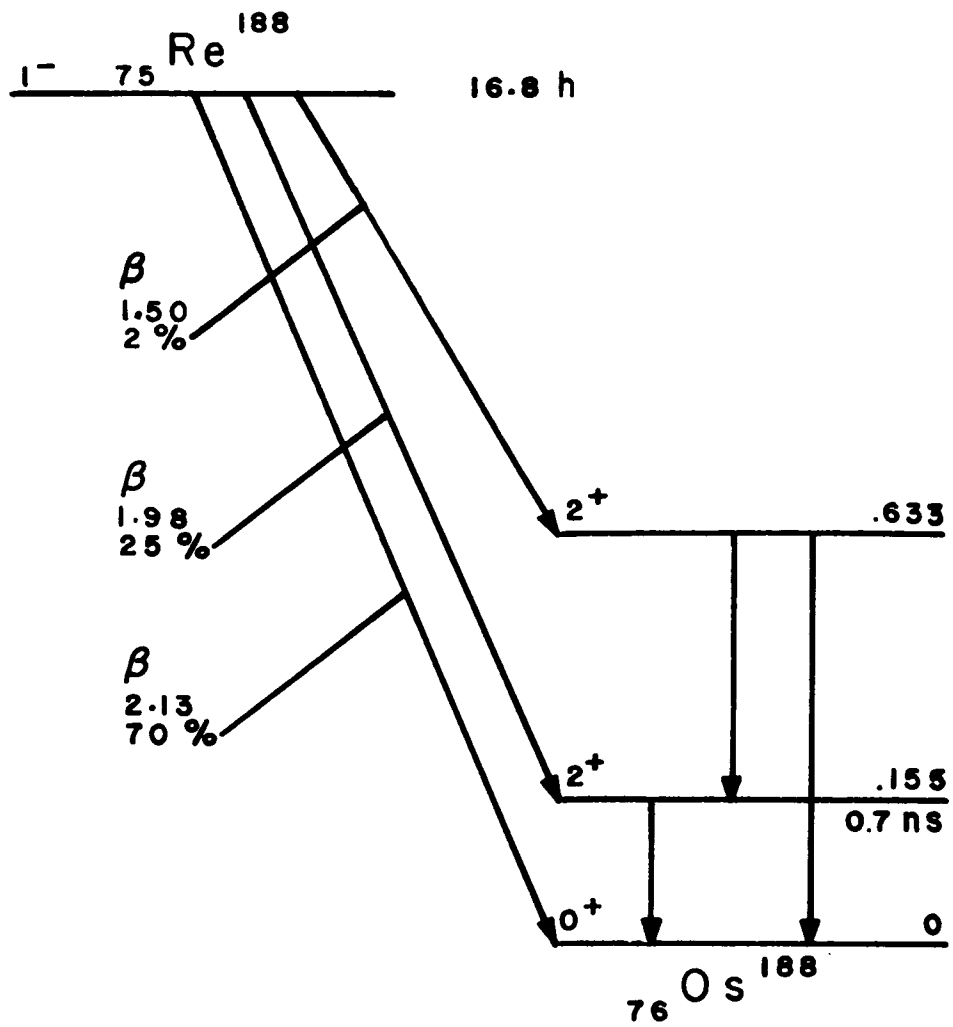


Fig. 10. Principal branches of decay scheme of Re^{188} .

The Co^{60} source was deliberately off-centered (a 7% difference in the gamma singles rates for the 180° and 90° (270°) positions was produced) in order to simulate less than optimum conditions for the measurement. Since the beta decay of the Co^{60} nucleus is "Allowed", the beta gamma correlation should be isotropic i.e., a determination of the A_2 -coefficient should yield $A_2 = 0$. Any deviation from isotropy would indicate a deficiency in the experimental technique or the presence of faulty equipment. The directional correlation in Co^{60} gave:

$$A_2 = -0.0003 \pm 0.006 \text{ (}\gamma\text{-2 Probe)}$$

$$A_2 = +0.005 \pm 0.007 \text{ (}\gamma\text{-1 Probe)}$$

The isotopes Re^{185} (96.7% Re^{185} + 3.3% Re^{187}) and Re^{187} (99.2% Re^{187} + 0.8% Re^{185}) were purchased from the Oak Ridge National Laboratory in separated form. The Rhenium metals, in the form of a powder, were sealed in quartz vials and irradiated in the reactor at McMaster University at a flux of about 10^{13} neutrons per cm^2 per second. The $n\text{-}\gamma$ reaction in Rhenium leads to 90 hr. Re^{186} and 17 hr. Re^{188} . Irradiation of a given sample was terminated upon reaching an activity of 4 mc./mg. The vials were crushed under nitric acid and the resulting solution evaporated to dryness in a beaker. The residue was then dissolved in a few drops of water and the resulting solution evaporated to dryness in a tantalum evaporation crucible. The crucible was placed in the Balzer (Type MBA 3) evaporation unit and centered with respect to a 5 mm. in diameter opening in a brass mask set directly above it. The source backing, a thin Al foil 0.0003" thick, was positioned on the mask. The temperature of the crucible was then raised slowly and the Rhenium compound evaporated

and deposited uniformly on the foil within a circular area 5 mm. in diameter at the center of the foil. All sources were thin enough to be transparent (20-50 $\mu\text{g./cm.}$) and therefore source scattering effects were deemed to be negligible. Several different sources of each radioactive isotope were used during the course of the directional correlation measurements.

The source position and the gamma detectors were properly centered. The fast-slow coincidence circuit was adjusted as described in Chapter IV.

The Re^{188} was run with the single channel analyzer in the gamma channel set on the 155-Kev gamma photopeak with a window a width selected differentially so as to reject the Os K X-ray contribution. Fig. 11 is a plot of the gamma spectrum. The single channel analyzer in the beta channel was set to discriminate against noise. Angular positioning and recording of data were accomplished automatically, usually at 4-10 minute intervals. At each beta energy the sequence 90° - 180° (γ -2 Probe), 180° - 270° (γ -1 Probe) was scanned forward and backward many times. The triple coincidences, gamma singles and beta singles were recorded at each position.

The Re^{186} was run with the single channel analyzer in the gamma channel set on the 137-Kev gamma photopeak with a window width selected differentially so as to reject the Os and W K X-ray contribution. Fig. 12 is a plot of this gamma spectrum. The general procedure was the same as that used for the Re^{188} except that standard counting times were extended to incorporate 4-30 minute intervals. It is noted here that no work was

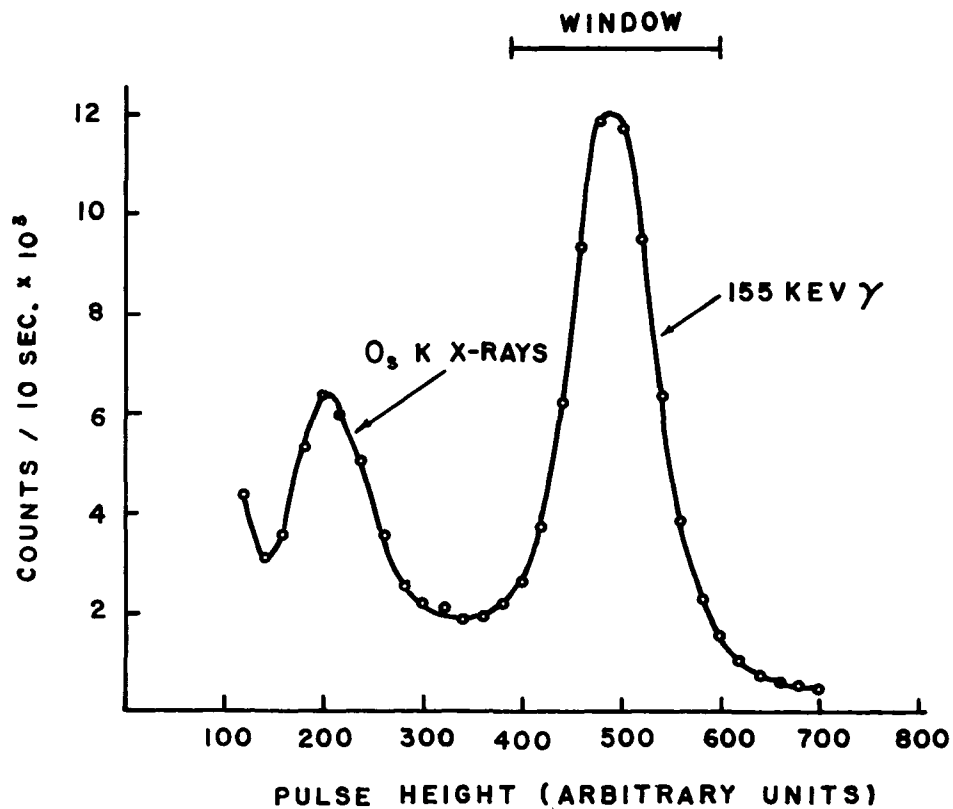


Fig. 11. Low energy gamma pulse height distribution from Re^{188} .

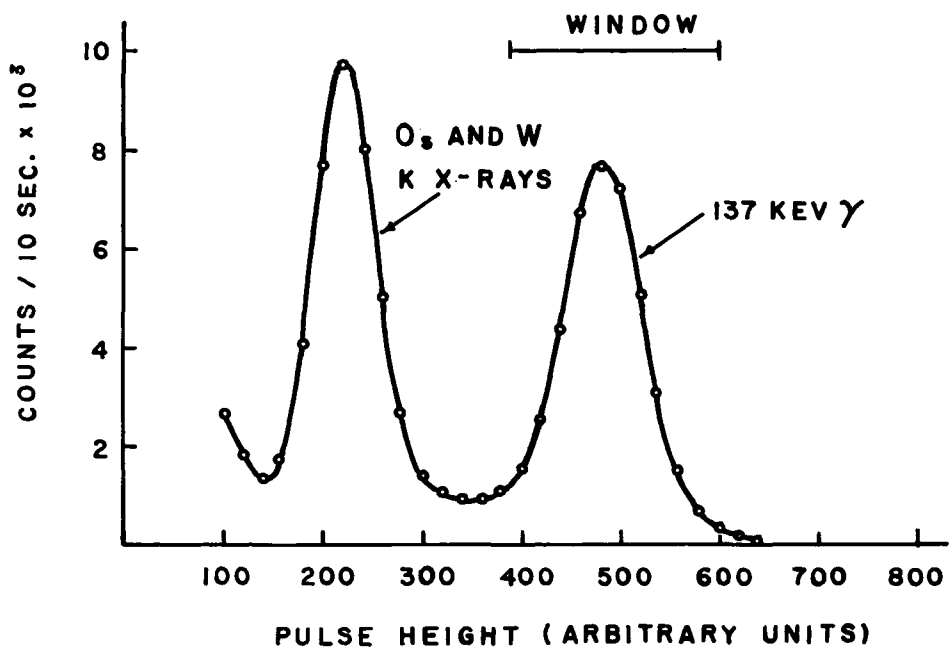


Fig. 12. Low energy gamma pulse height distribution from Re^{186} .

done on the Re^{186} samples until a few days after such sources had been made up. This procedure allowed for the reduction of the 17 hr. Re^{188} activity to negligible proportions relative to the 90 hr. Re^{186} activity.

In the experiments on Re^{186} and Re^{188} , the maximum analyzed beta and gamma singles rates were 400,000 counts/min. and 500,000 counts/min. respectively. Each energy was examined a number of times. A total of about 200,000 true coincidences was obtained at each energy. The ratio of true/chance coincidences exceeded 7 at all energies.

The chance rate N_c was monitored regularly in the course of each experiment. The resolving time 2τ was determined from the relation $[2\tau = N_c/N_\beta N_\gamma]$ and found to be constant within $\pm 6\%$. No dependence of 2τ on beta energy was observed. The variation in resolving time obtained from an actual run on the Re^{186} isotope is presented in Table II.

TABLE II

The Variation in Resolving Time 2τ for a β - γ Directional Correlation Run in Re^{186} .

W	2τ (nsec.) (γ -1 Probe)	2τ (nsec.) (γ -2 Probe)
1.6	14.1 ± 0.4	20.2 ± 0.4
1.8	14.9 ± 0.7	21.2 ± 0.5
2.0	14.2 ± 0.5	20.3 ± 0.4
2.2	15.6 ± 0.6	20.1 ± 0.4
2.4	15.6 ± 0.4	21.0 ± 0.4
2.6	13.8 ± 0.6	22.1 ± 0.5

The electronic circuits for the beta and gamma channels proved to be very stable. Correction for the small variation in gamma solid angle θ (due to imperfect location of the source on the rotation axis) and for radioactive decay of the sample was made by normalizing the coincidence counts to the gamma singles rates.

The possibility of a gamma-gamma scattering contribution to the coincidence count rate was investigated. The procedure consisted of closing the spectrometer baffle and observing the coincidence rate under normal experimental conditions. No significant scattering effect was detected.

C. Treatment of Data

The true coincidence rates were derived from the formula

$$W(\theta) = (T - N_c) / N_\gamma \quad (24)$$

where: θ = beta gamma detection angle

T = observed coincidence rate

N_c = chance rate = $2\tau N_\beta N_\gamma$

N_γ = gamma singles rate (normalizing factor)

N_β = beta singles rate

In the directional correlation experiments the "anisotropy"

A given by:

$$A = \frac{W(\pi)}{W(\pi/2)} - 1 \quad (25)$$

was determined for each counting cycle of 90° - 180° (γ -2 Probe) and 180° - 270° (γ -1 Probe) where the 90° and 270° positions are geometrically equivalent. The anisotropy A is related to the A_2 coefficient in the

expression $[W(\theta) = 1 + f_2 A_2 P_2(\cos \theta)]$ by the equation:

$$f_2 A_2 = \frac{2A}{3 + A} \quad (26)$$

i.e.
$$A_2 = \frac{1}{f_2} \left(\frac{2A}{3 + A} \right) \quad (27)$$

The average value of the anisotropy, \bar{A} , was determined at each energy. This value is a weighted average, the weight factor consisting of the inverse of the fractional standard deviation squared. The A_2 coefficient at each energy is then given by:

$$A_2 = \frac{1}{f_2} \left(\frac{2\bar{A}}{3 + \bar{A}} \right) \pm \bar{\sigma} \quad (28)$$

where $\bar{\sigma}$ is the Standard Deviation in A_2 due to statistical effects. Its magnitude was obtained in the usual manner from the theory of propagation or errors.

The f_2 correction factors obtained were:

$$f_2 = f_2(e^-) f_2(\gamma) = 0.725 \times 0.957 = 0.694 \pm 0.003 \quad (\gamma\text{-2 Probe})$$

$$f_2 = f_2(e^-) f_2(\gamma) = 0.725 \times 0.967 = 0.701 \pm 0.003 \quad (\gamma\text{-1 Probe})$$

where the source to crystal distance in each case was 10 cm.

The values of the A_2 coefficients obtained for the beta gamma directional correlation in Re^{188} are presented in Table III; the values of A_2 obtained for the directional correlation in Re^{186} are presented in Table IV.

TABLE III
The Values of the A_2 Coefficients Obtained For The
 β - γ Directional Correlation in Re^{188}

Energy (W)	A_2 (γ -1 Probe)	A_2 (γ -2 Probe)	A_2 (Average)
3.01	0.141 ± 0.014	0.133 ± 0.013	0.133 ± 0.005
	0.130 ± 0.014	0.129 ± 0.015	
		0.141 ± 0.010	
		0.130 ± 0.011	
		0.124 ± 0.011	
3.22	0.163 ± 0.013	0.140 ± 0.009	0.151 ± 0.004
	0.152 ± 0.010	0.160 ± 0.008	
		0.135 ± 0.009	
3.42	0.159 ± 0.016	0.160 ± 0.010	0.161 ± 0.006
	0.159 ± 0.015	0.156 ± 0.013	
		0.171 ± 0.014	
3.61	0.164 ± 0.014	0.169 ± 0.009	0.176 ± 0.004
	0.201 ± 0.015	0.158 ± 0.009	
	0.180 ± 0.010	0.193 ± 0.013	
		0.168 ± 0.013	
3.81	0.183 ± 0.010	0.176 ± 0.011	0.183 ± 0.006
		0.187 ± 0.009	
4.01	0.198 ± 0.010	0.196 ± 0.014	0.201 ± 0.004
	0.208 ± 0.010	0.197 ± 0.009	
		0.203 ± 0.009	
4.21	0.209 ± 0.014	0.222 ± 0.012	0.216 ± 0.006
	0.216 ± 0.013	0.215 ± 0.012	

TABLE IV
The Values of the A_2 Coefficients Obtained For The
 β - γ Directional Correlation in Re^{186}

Energy (W)	A_2 (γ -1 Probe)	A_2 (γ -2 Probe)	A_2 (Average)
1.60	0.035 ± 0.009 0.033 ± 0.009 0.046 ± 0.010	0.051 ± 0.009 0.039 ± 0.008 0.046 ± 0.010	0.043 ± 0.004
1.80	0.060 ± 0.009 0.058 ± 0.009 0.059 ± 0.009	0.048 ± 0.008 0.069 ± 0.008 0.044 ± 0.008	0.059 ± 0.004
2.00	0.079 ± 0.009 0.077 ± 0.009 0.078 ± 0.010	0.083 ± 0.008 0.068 ± 0.008 0.085 ± 0.009	0.079 ± 0.004
2.20	0.076 ± 0.009 0.096 ± 0.009 0.098 ± 0.010	0.078 ± 0.008 0.081 ± 0.008 0.066 ± 0.009	0.085 ± 0.004
2.40	0.098 ± 0.009 0.098 ± 0.010	0.089 ± 0.008 0.107 ± 0.009	0.098 ± 0.004
2.60	0.093 ± 0.010	0.093 ± 0.009	0.093 ± 0.006

CHAPTER VI
MAGNETIC AND QUADRUPOLE INTERACTIONS IN
 Re^{186} AND Re^{188} ANGULAR CORRELATIONS

A. Introduction

In the beta gamma correlation measurements reported in Chapter V, it was assumed that the angular correlation function $W(\theta)$ was of the form $[W(\theta) = 1 + f_2 A_2 P_2(\cos \theta)]$ which implies an unperturbed correlation. However, depending on the source conditions, the angular correlation can be more or less attenuated due to a static quadrupole interaction and/or a time-dependent coupling caused by the after-effects of hole formation. The attenuation can be expressed by an attenuation factor G . Thus a more general expression for the angular correlation function $W(\theta)$ would be:

$$W(\theta) = 1 + f_2 G_2 A_2 P_2(\cos \theta) \quad (29)$$

where $G_2 \leq 1$.

The experiments discussed in this chapter were undertaken to determine the possible existence of any attenuation effects due to perturbations of the intermediate state in the beta gamma cascades of Re^{186} and Re^{188} . The Re^{186} isotope was chosen for this investigation because of its relatively long half-life of 90 hrs. Due to the very strong similarity in the isotopes Re^{186} and Re^{188} it is expected that any attenuation effects present in the beta gamma cascade of Re^{186} will also

be present in the Re^{188} cascade.

B. Magnetic Decoupling Experiment

If the directional correlation suffers an attenuation due to a magnetic hfs interaction, i.e., a coupling between the nuclear spin I and the spin of the atomic shell J , then it should be possible to decouple I and J with the aid of an external magnetic field applied in the direction of emission of the beta rays (longitudinal decoupling). A field of a few thousand gauss should be quite sufficient to achieve complete decoupling.

A magnet of the electron lens type, easily giving a sufficiently strong and also well confined field was built for the decoupling experiment. A schematic of the decoupling lens and of the experimental arrangement used in the magnetic decoupling experiment is shown in Fig. 13.

Square section copper wire was wound on a brass cylinder whose inner diameter was cut in the shape of a cone to permit detection of gamma radiation in the 180° position. During the winding operation a constant tension was maintained on the wire and each turn was pressed alongside the previous one, without leaving any visible gap. At the end of each row the "fly-over" was brought over smoothly to the next row. Each row was covered with a thin film of a high thermal conductivity insulating epoxy glue. Water cooling for the coils was provided for by means of a water channel milled out of the brass cylinder. Additional cooling was provided by attaching the neck of the lens to a thick

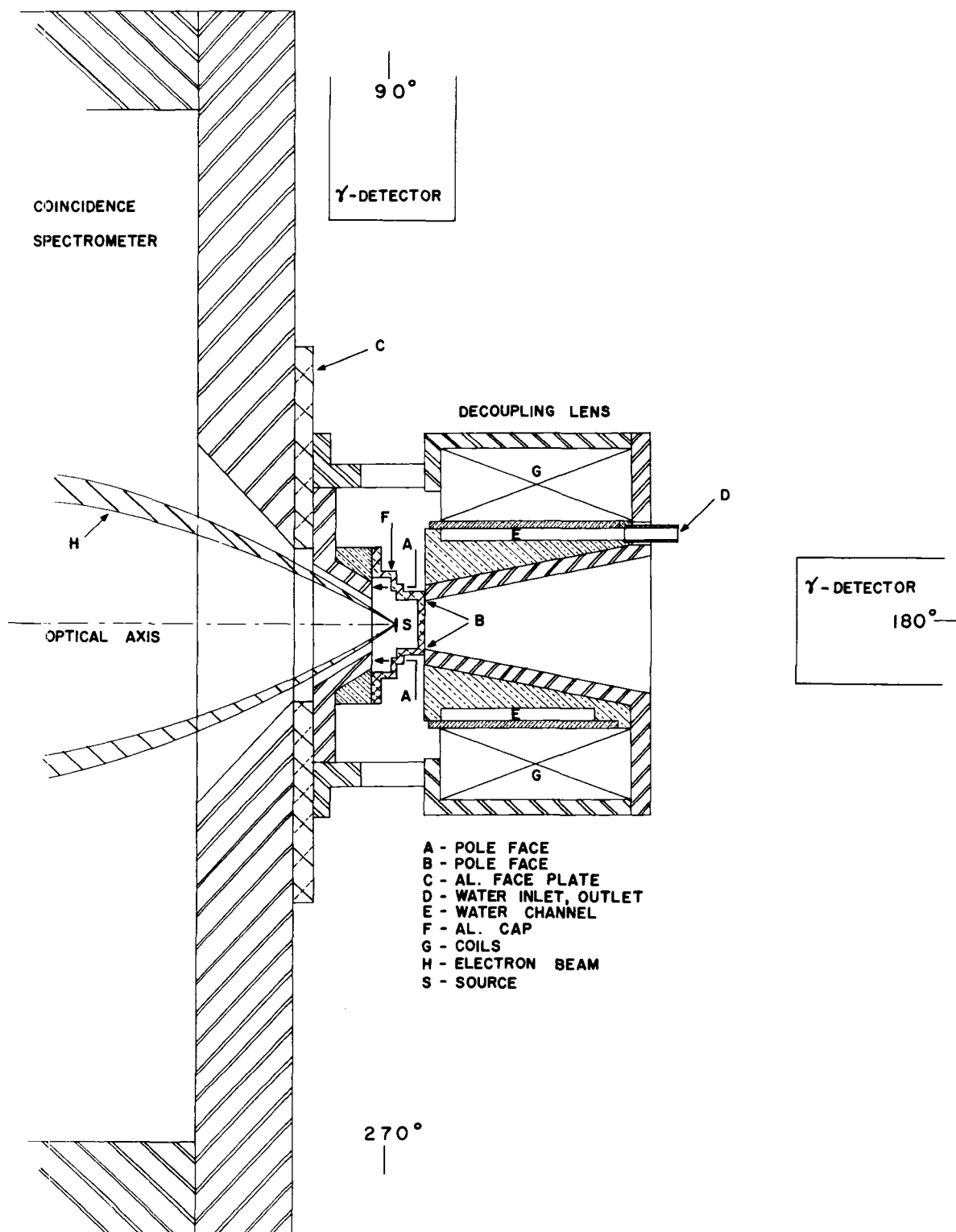


Fig. 13. Schematic of the decoupling lens and of the experimental arrangement used in the magnetic decoupling experiment.

aluminum face plate which fits onto the source facing surface of the spectrometer iron flange thus resulting in a coupling of the spectrometer cooling system to the magnetic lens. Circular openings were cut in the neck of the lens to permit counting at the 90° and 270° positions.

The pedistal source holder was removed from the coincidence spectrometer in order to accommodate the lens. A new source holder consisting of an aluminum cap, machined to accept the aluminum source rings was constructed. This cap was mounted between the two pole faces A and B. The position of the source in the lens was made to coincide with the previous pedistal source position. The geometry of the lens is such that electrons leaving the source enter the spectrometer via paths free of mechanical obstructions. Vacuum tight seals were made between the source holder and the pole face A, between the pole piece A and the aluminum face plate, and between the face plate and the spectrometer by means of O-rings.

The current versus magnetic field response of the decoupling lens is given in Fig. 14. Preliminary tests showed that a field of 3-KG. (≈ 40 Amps.) could be maintained for an indefinite period of time without exceeding the permissible operating temperature of the magnet wire.

A necessary requirement for the decoupling magnet producing the external field is that its influence on the electron trajectories should be small. The 624-Kev Ba^{137} electron conversion line was scanned in the beta spectrometer at field strengths of 0-KG. and 3-KG. in the decoupling lens. The profiles are indicated in Fig. 15. The results indicate that a field of 3-KG. from the decoupling lens does not influence

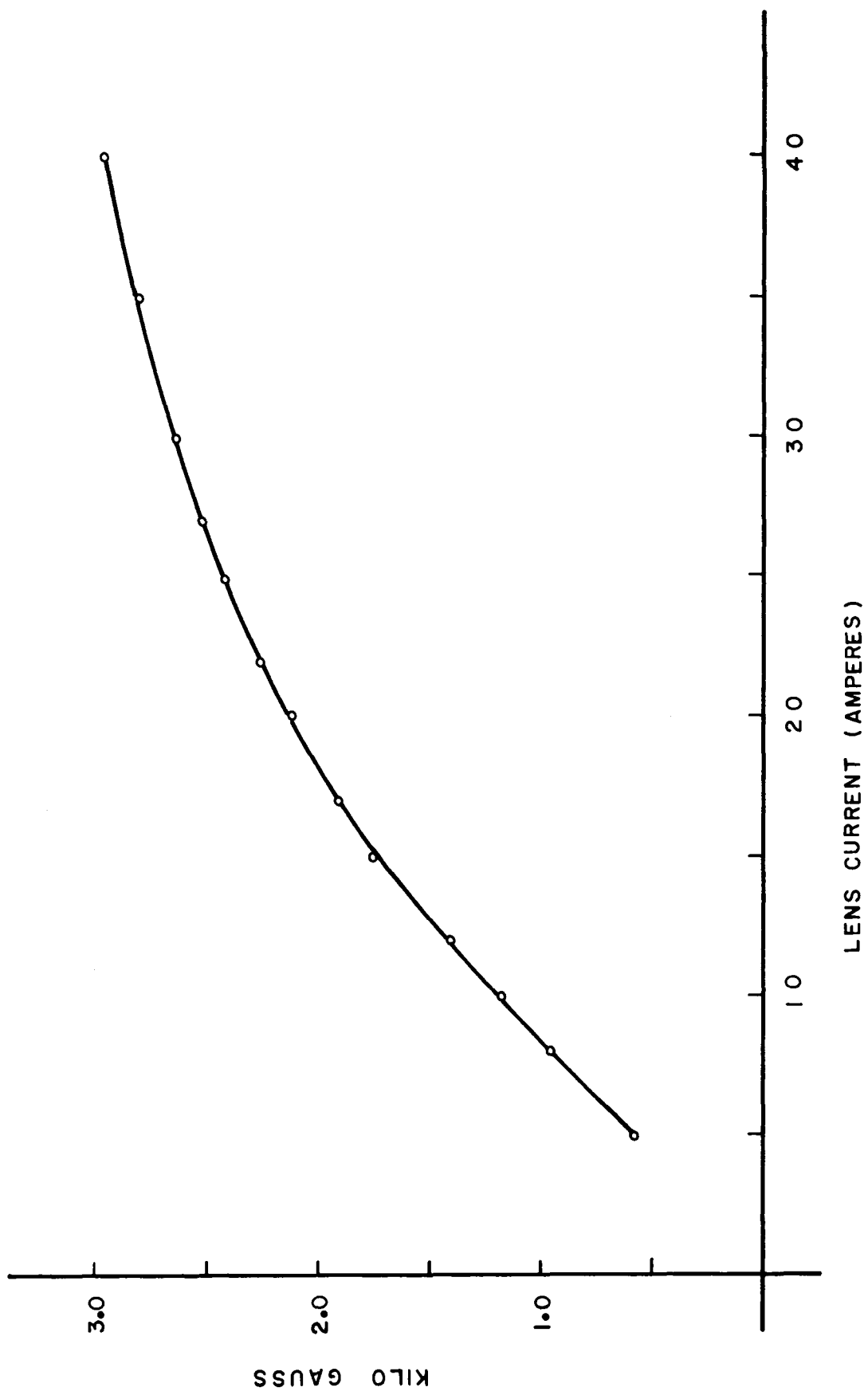


Fig. 14. Plot of current versus magnetic field for the decoupling lens.

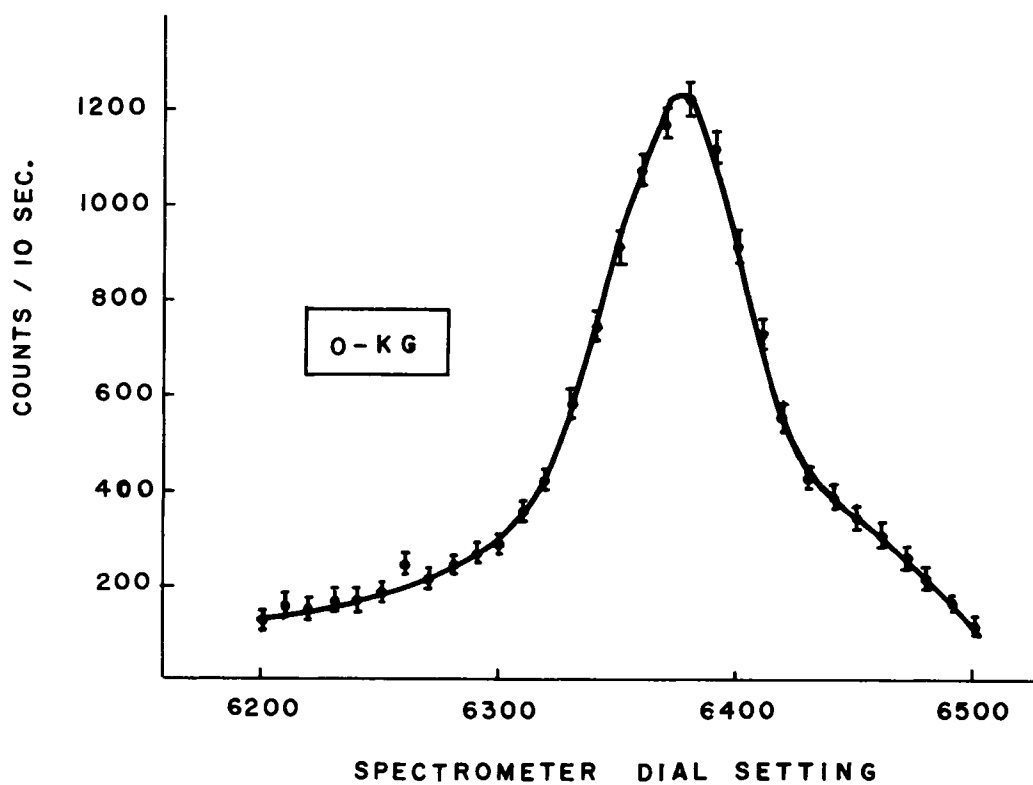
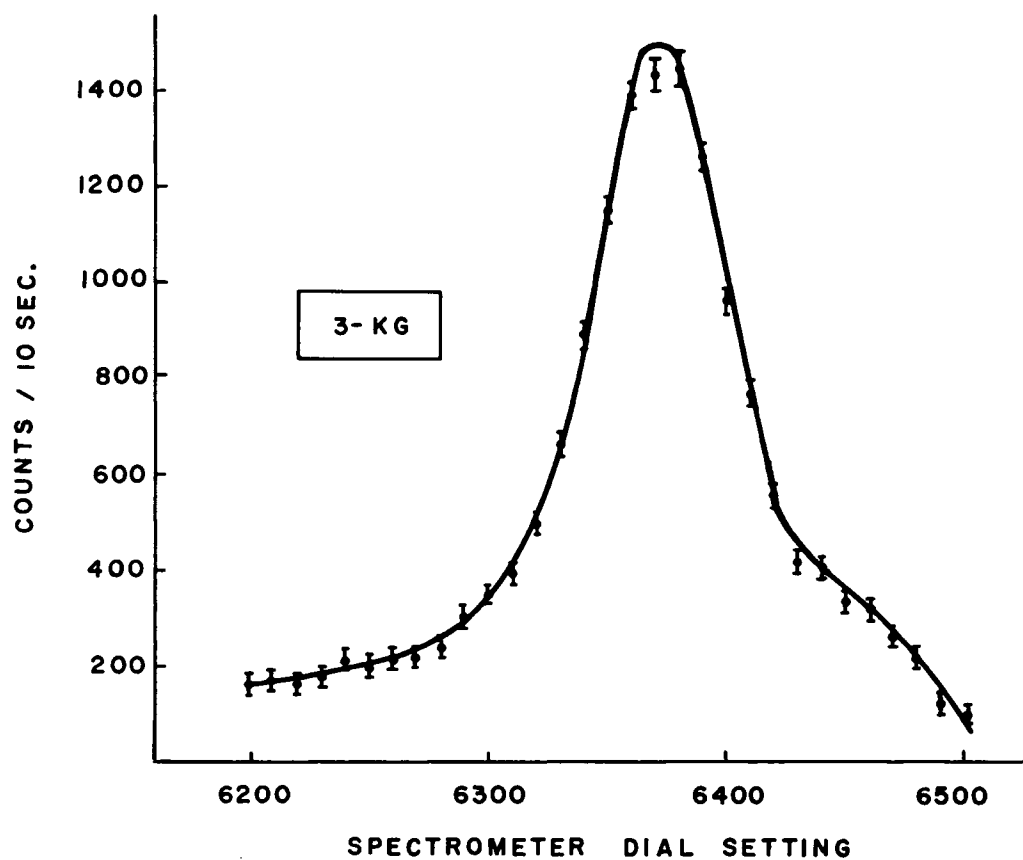


Fig. 15. Profiles of the 624-Kev Ba^{137} electron conversion line for 0-KG and 3-KG fields in the decoupling lens.

the spectrometer resolution but does give an increase in the spectrometer transmission of about 15% due to a deflection of electrons with emission angles larger than those normally accepted into the spectrometer aperture cone. This increase in transmission implies a possible difference between the geometrical correction factor $f_2(e^-)$ obtained with the "FIELD-ON" (3-KG.) and with the "FIELD-OFF" (0-KG.). A determination of $f_2(e^-)$ however, for the "FIELD-ON" and for the "FIELD-OFF" gave identically $f_2(e^-) = 0.741 \pm 0.003$. The slight shift in the peak position (Fig. 15) corresponds at most to a change of 2-Kev in the electron energy calibration which, for our purposes, is insignificant. Further experimental tests revealed that the 3-KG. field did not influence the γ -1 probe but had a pronounced effect on the γ -2 probe. In view of this, it was decided not to utilize the γ -2 probe for measurements in the presence of an external magnetic field. Finally, it is noted here that gamma scattering in the decoupling lens could lead to incorrect experimental results. However, for the magnetic decoupling experiment, in which a comparison of the A_2 coefficient with the "FIELD-ON" and "FIELD-OFF" was made, the scattering effect, if present, should be of little importance to the interpretation of the results.

The general procedure adopted for the decoupling experiment was essentially the same as that used for the directional correlation measurements described in Chapter V. Due to the physical dimensions of the decoupling lens, the gamma counters had to be moved back an additional 4 cm. from the source to permit their free rotation on the angular correlation table. This displacement meant a change in the

correction factor $f_2(\gamma)$. The new values for $f_2(\gamma)$ were found to be:

$$f_2(\gamma) = 0.982 \quad (\gamma-1 \text{ Probe})$$

$$f_2(\gamma) = 0.974 \quad (\gamma-2 \text{ Probe})$$

Thus we have:

$$f_2 = f_2(e^-)f_2(\gamma) = 0.741 \times 0.982 = 0.727 \pm 0.003 \quad (\gamma-1 \text{ Probe})$$

$$f_2 = f_2(e^-)f_2(\gamma) = 0.741 \times 0.974 = 0.721 \pm 0.003 \quad (\gamma-2 \text{ Probe})$$

The angular correlation measurements were made at one energy only, namely at $W = 2.0$.

In contrast to the metal Al source backing used for the angular correlation measurements in Chapter V, the decoupling experiment was conducted utilizing an insulator (Mica) source backing. Thus, if a magnetic interaction is present, a maximum attenuation should be displayed in the absence of an external magnetic field.

Measurements were made with the "FIELD-ON" and the "FIELD-OFF". The results are presented in Table V where it is easily seen that within statistics:

$$A_2(\text{FIELD-ON; Mica}) = A_2(\text{FIELD-OFF; Mica}) = 0.066 \pm 0.003$$

In Chapter V, however, it was found that $A_2(W = 2.0; \text{Al}) = 0.079 \pm 0.004$. It is believed that this difference in A_2 values is probably due to gamma scattering from the decoupling lens. In order to test for the possibility of such an effect the angular correlation measurements, utilizing the decoupling lens, was repeated with an Al backed source. This measurement gave $A_2 = 0.068 \pm 0.003$. Thus, in all probability the attenuation of A_2 is due to γ scattering.

TABLE V

The Values of the A_2 Coefficient ($W = 2.0$) Obtained For the β - γ Directional Correlation in Re^{186} Utilizing the Magnetic Decoupling Lens

	A_2 (γ -2 Probe)	A_2 (γ -1 Probe)	A_2 (Average)
FIELD-ON	0.059 ± 0.008	0.078 ± 0.010	
	0.064 ± 0.007	0.065 ± 0.008	
	0.070 ± 0.007	0.067 ± 0.008	
	0.066 ± 0.007	0.068 ± 0.008	
	0.059 ± 0.007	0.073 ± 0.008	0.067 ± 0.003
FIELD-OFF		0.068 ± 0.009	
		0.060 ± 0.009	
		0.069 ± 0.009	
		0.060 ± 0.008	
		0.059 ± 0.008	
		0.052 ± 0.008	
		0.065 ± 0.008	
		0.066 ± 0.008	
		0.061 ± 0.008	
	0.071 ± 0.008	0.064 ± 0.003	

In summary, we have found that:

$$A_2(\text{FIELD-ON; Mica}) = A_2(\text{FIELD-OFF; Mica}) = A_2(\text{Al})$$

It is concluded then that no magnetic hfs interaction is displayed in the Re^{186} and hence also in the Re^{188} beta gamma cascades.

The quadrupole interaction, however, will give the usual quadrupole attenuation if present.

C. Electric Quadrupole Interaction

In order to determine whether a static quadrupole interaction attenuates the beta gamma angular correlations in Re^{186} and Re^{188} the multichannel delayed coincidence method employing the pulse overlap principle was utilized.

Consider that the excited state of the intermediate level of some double cascade is formed by a preceding decay. The preceding event provides us with a "preceding pulse" and the radiation by which the excited state decays to a lower state provides us with a "delayed pulse". The distribution of time delays between the two kinds of pulses can be measured by means of the delayed coincidence method. The preceding and delayed pulses are shaped to standard size and shape and fed to a time to amplitude converter (TAC) where they are allowed to overlap in time. The output from the converter is linearly proportional to the duration of overlap which in turn is linearly proportional to the relative delay of the two pulses. If the output from the TAC unit is coupled to a multichannel pulse amplitude analyzer the whole of the delay

distribution, or time spectrum, can be recorded in a single measurement. Fig. 16, where 0 is the centroid of the distribution, is a typical example of a time spectrum. The coincidences to the left of 0 are termed the "FAST" coincidences, those to the right of 0 the "DELAYED" coincidences, and the aggregate the "NORMAL" coincidences.

The possible presence of a static interaction in the beta gamma cascade of Re^{186} , where the beta particles constitute the preceding pulses and the 137-Kev gammas the delayed pulses, was investigated at a beta energy of $W = 2.0$. Aluminum backed sources were used.

Fig. 17 depicts the experimental arrangement. The fast limited pulses to the TAC unit (21) were shaped to a width of ≈ 40 nsec. and height ≈ 0.6 volts. The linear output from the TAC was fed simultaneously to the triple coincidence circuit and to the input of the 400 channel TMC kicksorter via a 2 μ sec. delay line which was used for timing purposes. The output from the triple coincidence unit was fed to a "Pulse Routing Gate" (22). The output from the latter circuit was used to gate the kicksorter operated in the coincidence mode. The "Pulse Routing Gate" permitted the time spectra due to the γ -2 (90° and 180° positions) and the γ -1 (180° and 270° positions) probes to be routed to separate 100 channel subgroups of the kicksorter. Four independent time spectra were thus accumulated.

For these measurements the γ -1 [(NaI(Tl)] crystal was replaced by a plastic scintillator because of its faster response time. However, the count rates, and consequently the statistics, obtained with this crystal proved totally inadequate and hence the results derived from the

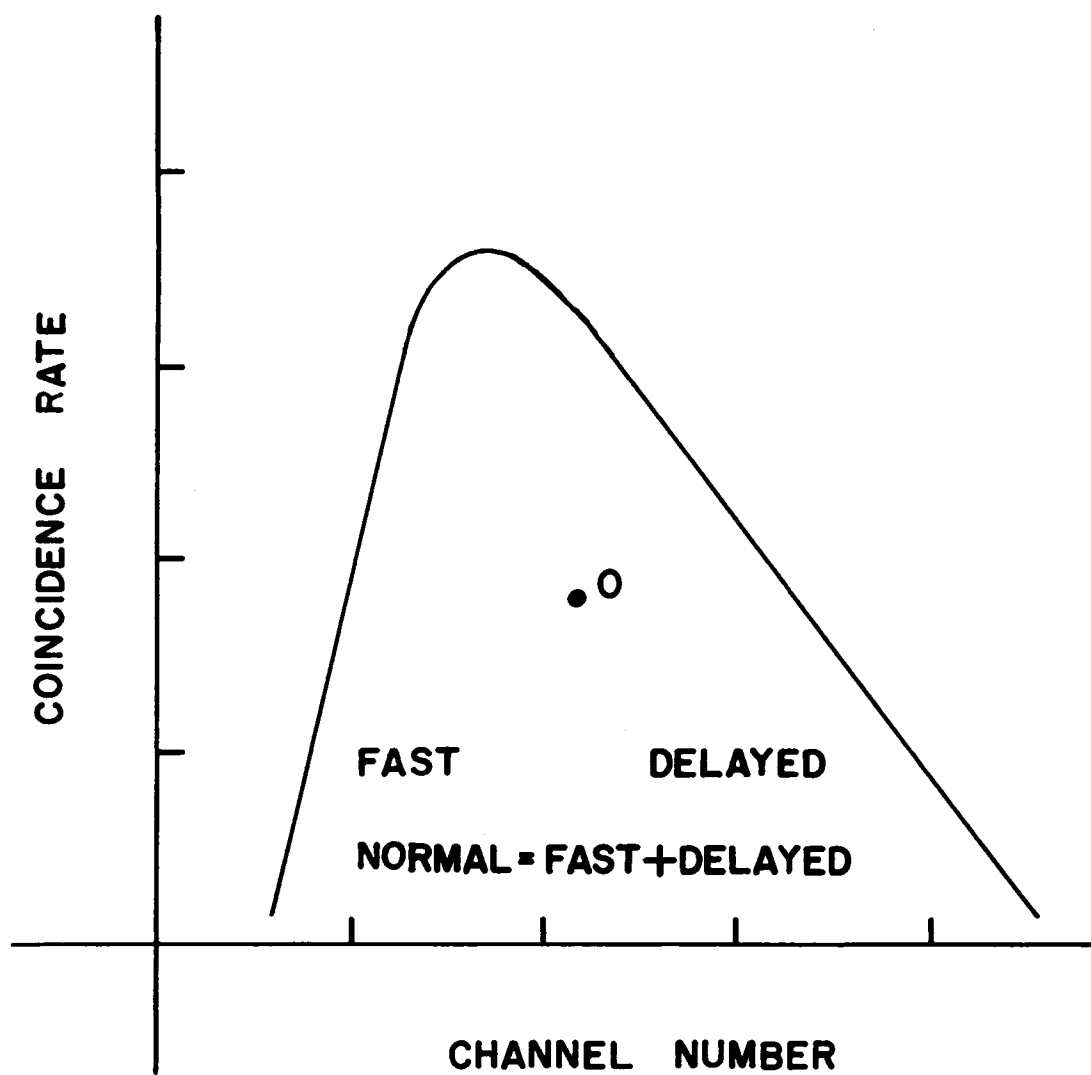


Fig. 16. A time spectrum.

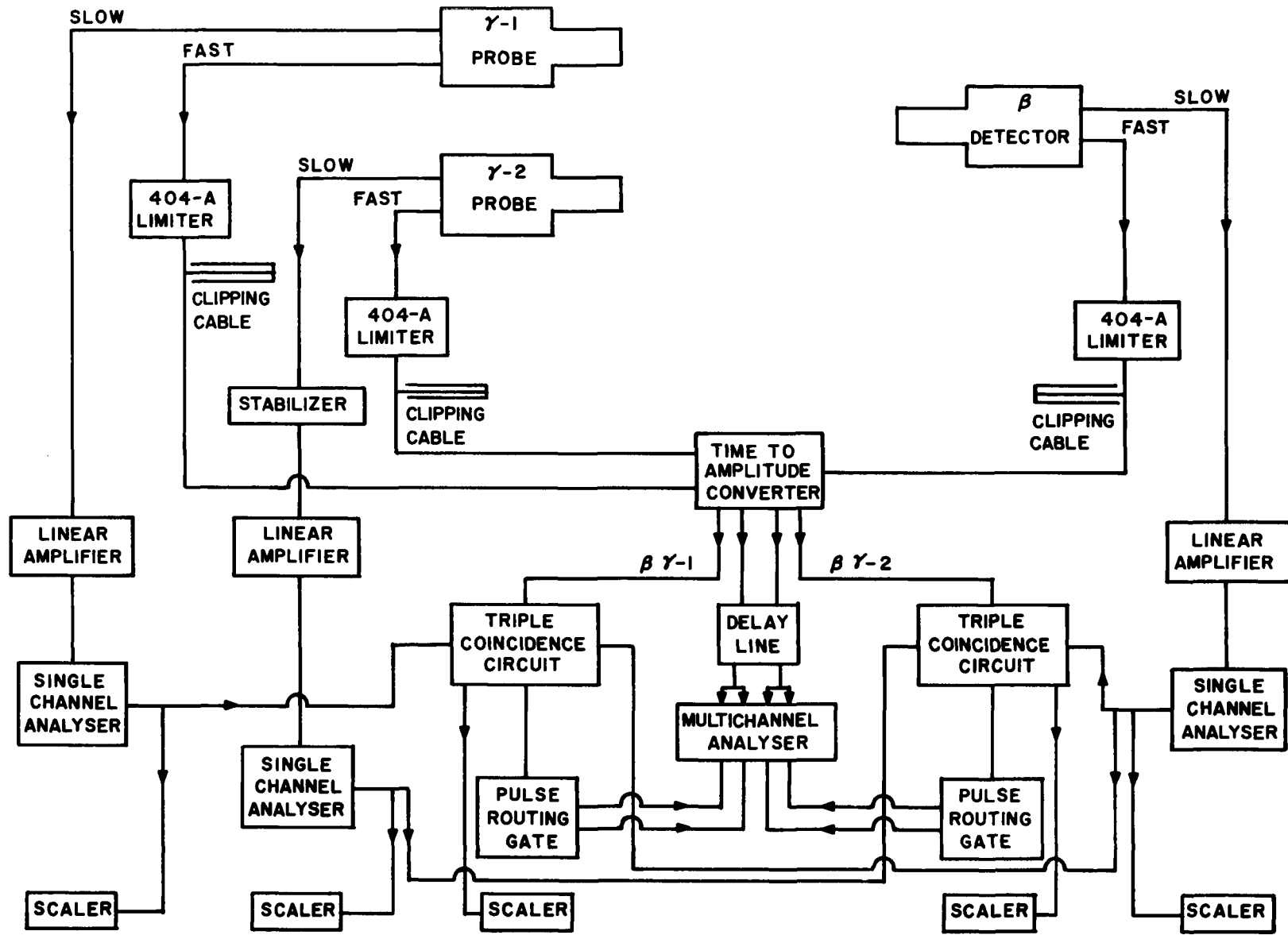


Fig. 17. Experimental arrangement for time spectra analysis.

γ -1 probe were discarded. The data obtained with the γ -2[NaI(Tl)] probe however were retained for analysis.

In order to assure operation within the linear region of the converter the beta pulses were delayed relative to the gamma pulses by approximately 24 nsecs. The time calibration of the converter was carried out by observing the time spectrum at several different measured lengths of cable. At each change of cable length the whole spectrum shifts by an observable amount on the pulse amplitude scale corresponding to the change in cable length. The time calibration thus obtained was 0.4 nsec. per kicksorter channel.

A separate determination of the chance rate was unnecessary since each time spectrum accumulated in the kicksorter consisted of the true delay distribution superposed upon a flat chance background.

In order to minimize the effect of drifts in the equipment, the time spectra data were punched out regularly and the kicksorter cleared and reset for a new accumulation of data. Fig. 18 depicts one of the time spectra, corrected for chance, obtained in these measurements.

The analysis of the data proceeded as follows. The time spectra for the 90° and 180° positions were corrected for the chance background. The centroid $\bar{0}$ for each distribution was calculated from the relation:

$$\bar{0} = \frac{\sum_t tF(t)}{\sum_t F(t)} \quad (30)$$

where t refers to the channel number and $F(t)$ refers to the coincidence rate in channel t . The error in $\bar{0}$ amounted at most to ± 0.02 channels. This value was determined by taking channel zero of the time spectra at

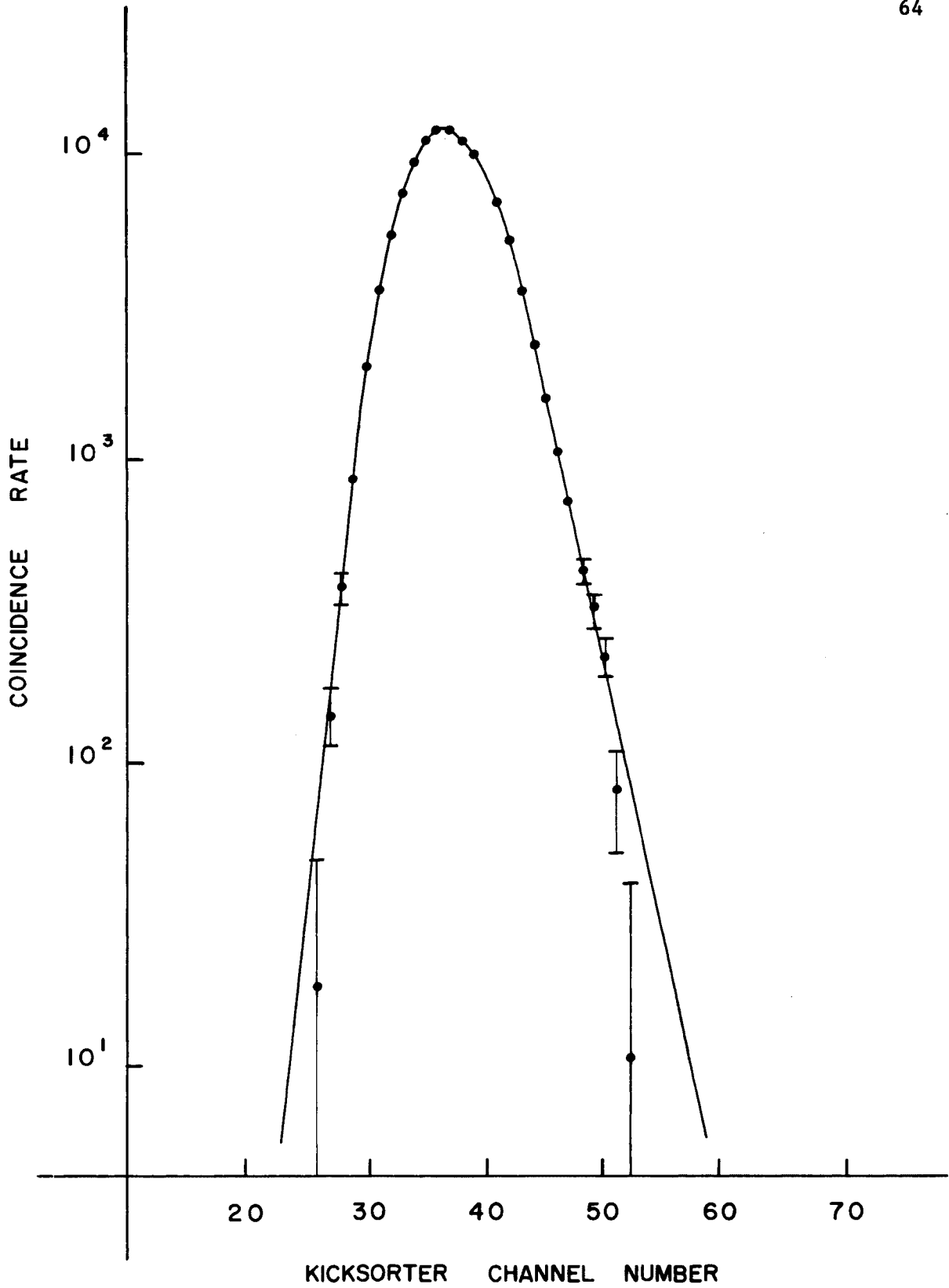


Fig. 18. Time spectrum for the β - γ cascade in Re^{186} Accumulated in the 90° position (run No. 1).

the approximate centroid position. The total number of FAST, DELAYED and NORMAL coincidences was determined at each angle. The values of $A_2(\text{FAST})$, $A_2(\text{DELAYED})$ and $A_2(\text{NORMAL})$ were determined for each run in the usual manner except that here $W(90^\circ)$ and $W(180^\circ)$, normalized to the gamma singles rate, refer to the properly selected coincidence counts from the time spectra. The values obtained for $A_2(\text{FAST})$, $A_2(\text{DELAYED})$ and $A_2(\text{NORMAL})$ are indicated in Table VI.

If a static quadrupole interaction is not present, then the following condition will be satisfied:

$$A_2(\text{FAST}) = A_2(\text{DELAYED}) = A_2(\text{NORMAL})$$

otherwise an attenuation due to a static interaction is indicated. The results of our measurements give:

$$A_2(\text{FAST}) = A_2(\text{DELAYED}) = A_2(\text{NORMAL})$$

The precision, however, with which these results can be quoted depends ultimately on the ability to separate the time spectra wholly into FAST and DELAYED portions. The shape of the time spectra is due to two effects: the lifetime of the intermediate level and the response of the equipment to prompt events. It is therefore very difficult to effect a total separation between FAST and DELAYED events. However, if it is assumed that the instrumental response is symmetrical about a point near the centroid, the prompt curve could be subtracted out of the spectrum leaving only DELAYED counts. If this analysis is carried out, then the precision of the data is approximately 20%. It is emphasized that this is a rough analysis but at least it indicates that no large attenuation due to a static quadrupole interaction occurs in the Re^{186} cascade

TABLE VI

Summary of Experimental Results Obtained From Time Spectra Analysis

Run	A_2 (FAST)	A_2 (NORMAL)	A_2 (DELAYED)
1	0.078 ± 0.008	0.081 ± 0.005	0.085 ± 0.008
2	0.071 ± 0.007	0.074 ± 0.005	0.079 ± 0.010
3	0.062 ± 0.008	0.065 ± 0.006	0.068 ± 0.011
4	0.080 ± 0.012	0.082 ± 0.008	0.086 ± 0.015
5	0.074 ± 0.011	0.070 ± 0.008	0.064 ± 0.014
AVERAGE	0.074 ± 0.004	0.076 ± 0.003	0.079 ± 0.005

and by inference in the Re^{188} cascade.

CHAPTER VII

SHAPE OF BETA SPECTRA IN THE DECAYS OF Re^{186} AND Re^{188}

A. Introduction

Most of the nonunique first forbidden transitions have a shape indistinguishable from the statistical shape, which is expected for the spectra of allowed transitions. It has been pointed out (1) however, that, in certain cases nonunique beta spectra may exhibit an energy dependent shape correction factor $C(W)$. Such deviations from the allowed shape are due to either the "cancellation effect" or to the "selection rule effect".

In the present investigation the spectra of the inner $1^- \rightarrow 2^+$ beta groups in the decays of Re^{186} and Re^{188} have been magnetically analyzed using the beta gamma coincidence technique. This study was undertaken in order to determine the shape of these inner beta groups. The Fermi plots for these transitions were derived from the relation

$$[N(\eta)/\eta^2 F(Z, \eta)]^{1/2} = \text{Constant} \cdot (W_0 - W) \quad (31)$$

where $F(Z, \eta)$ includes the correction for electron screening (23). (The Fermi functions used are due to Bhalla and Rose (24).

It was found that these beta groups have allowed shapes.

B. Experimental Procedure

The data obtained from the beta gamma directional correlation

measurements described in Chapter V were also utilized in the analysis of the shape of the spectra of the inner beta groups in Re^{186} and Re^{188} .

The experimental arrangement differed from the arrangement described in Chapter V only in the addition of a 400 channel TMC kicksorter used for the determination of the beta singles efficiency ω at each energy. Unlike the determination of the A_2 coefficient which involves a ratio such as $W(180^\circ)/W(90^\circ)$ and is therefore independent of the relative beta detection efficiency (the efficiencies cancel in the ratio) at each energy, the shape analysis involves single quantities only, such as $W(180^\circ)$ or $W(90^\circ)$, and not ratios, and is therefore sensitive to variations in ω for different energies. A knowledge of the relative beta singles efficiency over the energy range examined is therefore of the utmost importance.

A typical pulse height distribution for the beta particles is indicated in Fig. 19. The flat tail A is due to beta particles back-scattered from the plastic scintillator whereas the rise of the pulse height distribution at B is due to photomultiplier noise. In order to eliminate the noise, the beta discriminator must be set beyond the rise B. In so doing, we must inevitably lose some small fraction of the real pulses, the fraction lost depending on the beta energy. The singles efficiency ω , was computed by extrapolating the flat low tail on the pulse height distribution to zero amplitude. The beta pulse height distributions were recorded, at all beta energies analyzed, by the kicksorter operating in the coincidence mode: the slow beta pulses from

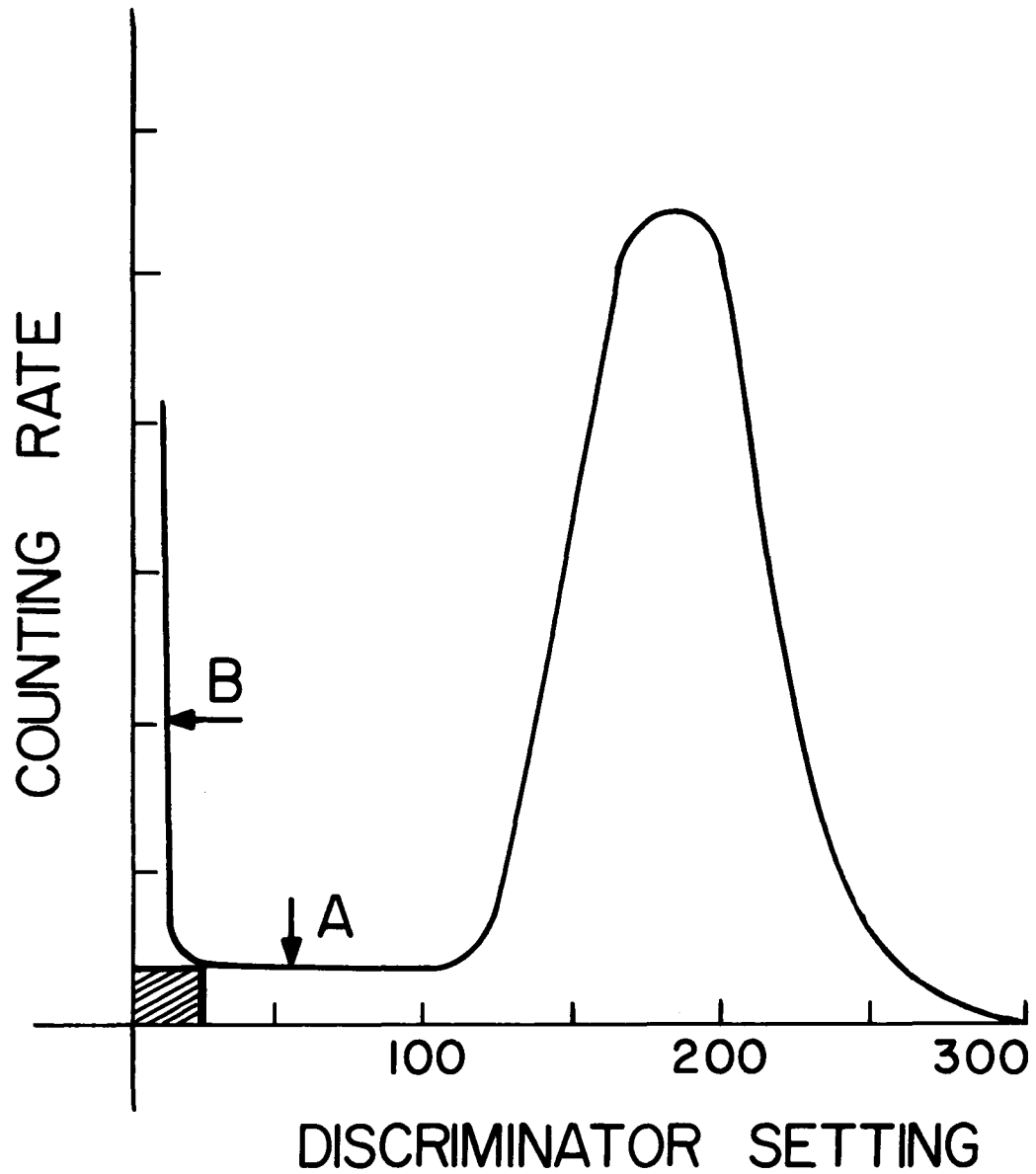


Fig. 19. Pulse height distribution for the beta particles focussed on the plastic scintillator in the beta spectrometer.

the beta detector were fed into the input of the kicksorter which was gated by the triple coincidences. The beta detection efficiency was found to increase by 3% over the energy range $W = 1.6$ to $W = 2.6$ for the (935-Kev beta) (137-Kev gamma) cascade in Re^{186} . A change of 2% in ω over the energy range $W = 3.0$ to $W = 4.4$ was recorded for the (1980-Kev beta) (155-Kev gamma) cascade in Re^{188} .

C. Treatment of Data

The coincidence data for the γ -1 (180° ; 270°) and γ -2 (90° ; 180°) probes, corrected for chance and normalized to the gamma singles rates, were combined to give $W(135^\circ)$, since:

$$W(90^\circ) + W(180^\circ) = 2W(135^\circ) \quad (\gamma\text{-2 Probe}) \quad (32)$$

$$W(270^\circ) + W(180^\circ) = 2W(135^\circ) \quad (\gamma\text{-1 Probe}) \quad (33)$$

The average value of $W(135^\circ)$ was determined at each energy.

The uncorrected value of $N(\eta)$ in equation(31) is then given by $[N(\eta) = W_{\text{av.}}(135^\circ)/\eta]$. In addition to the correction for the beta singles efficiency ω , $N(\eta)$ was also corrected for the beta gamma angular correlation in order to derive the integrated over 4π solid angle spectral shape. For the Re^{186} spectrum the latter correction amounted to about -1% at $W = 1.6$ and increased to -2% at $W = 2.6$; for the Re^{188} spectrum the correction amounted to about -3% at $W = 3.0$ and increased to -5% at $W = 4.4$.

D. Results

The Fermi plots obtained using the γ -1 and γ -2 probes were found to agree well with one another for both the Re^{186} and Re^{188}

beta spectra.

Fig. 20 is the Fermi plot of the $1^- \rightarrow 2^+$ beta spectrum of Re^{186} . The data fall on a statistically straight line; the shape correction factor is found to be constant to within $\pm 1\%$. The two sets of data give a final value of $(947 \pm 5)\text{Kev}$ for the extrapolated end point energy.

Fig. 21 is the Fermi plot of the $1^- \rightarrow 2^+$ beta spectrum of Re^{188} . The data fall on a statistically straight line; the shape correction factor is found to be constant to within $\pm 1.5\%$. The extrapolated end point energy gives a final value of $(1998 \pm 10)\text{Kev}$.

The results indicate that the beta spectra feeding the first excited states in Os^{186} and Os^{188} exhibit the statistical (allowed) shape.

For a comparison of the end point energies obtained in this investigation with those obtained by other authors refer to Table VII. The consistently lower values obtained by Johns et al (9) are probably due to the subtraction method that they employed in their analysis.

TABLE VII

A Tabulation of End Point Energies for Re^{186} and Re^{188}

Re^{186}	Re^{188}	Reference
$934.3 \pm 1.3 \text{ Kev}$		6
$927 \pm 2 \text{ Kev}$	$1961 \pm 2 \text{ Kev}$	9
$937 \pm 14 \text{ Kev}$	$1982 \pm 31 \text{ Kev}$	8
	$1998 \pm 5 \text{ Kev}$	25
$947 \pm 5 \text{ Kev}$	$1998 \pm 10 \text{ Kev}$	This Investigation

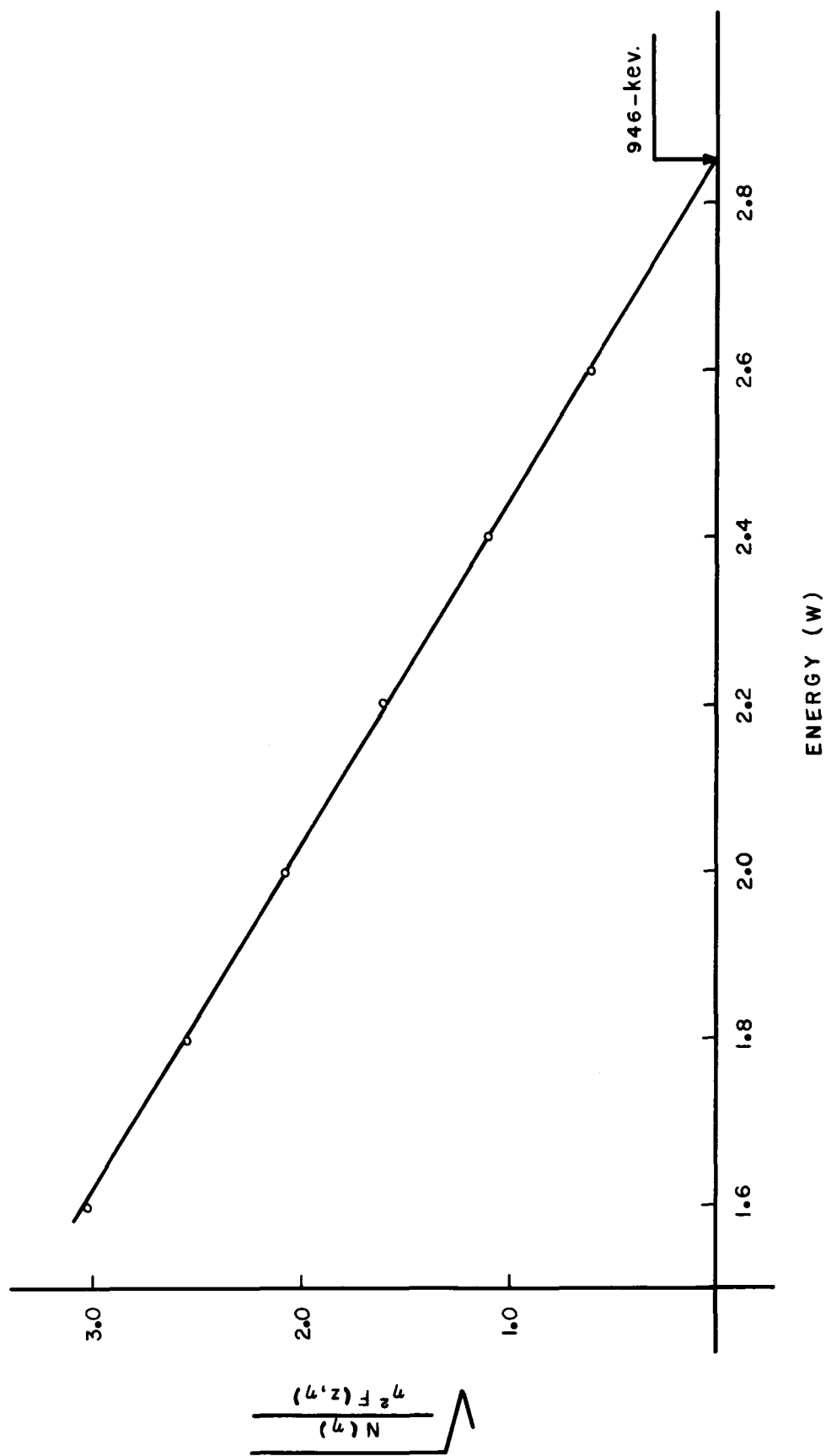


Fig. 20. Fermi plot of the inner beta spectrum of Re^{186} .

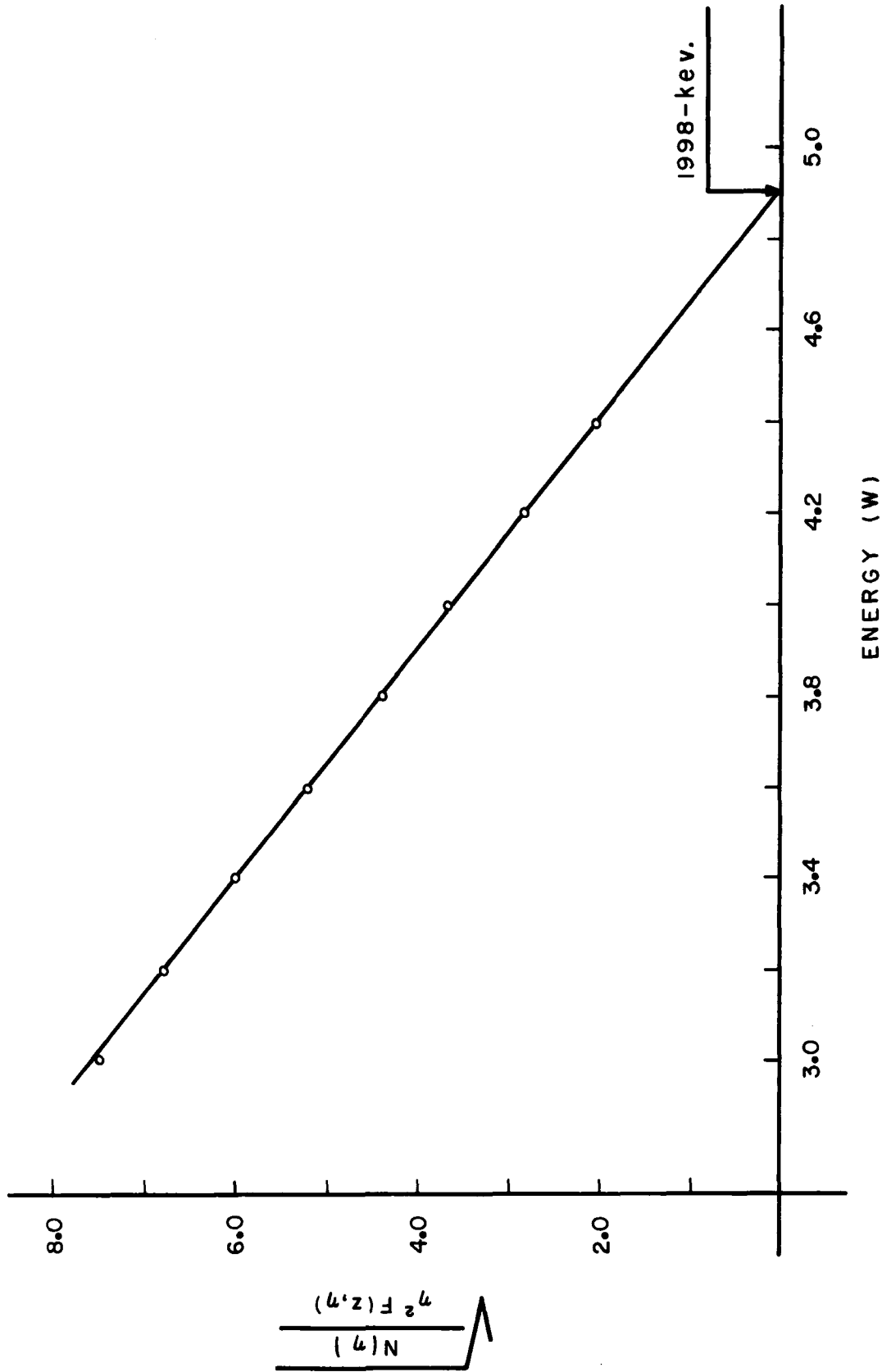


Fig. 21. Fermi plot of the inner beta spectrum of Re^{188} .

CHAPTER VIII

DETERMINATION OF NUCLEAR MATRIX ELEMENT PARAMETERS IN THE FIRST-FORBIDDEN BETA DECAY OF Re^{186} AND Re^{188}

A. Introduction

The experimentally determined functions $C(W)$ and $A_k(W)$ for Re^{186} and Re^{188} were compared with the theoretically predicted functions $C(W)$ and $A_k(W)$ computed for various combinations of the nuclear matrix element parameters Y , u and x (It is noted here that, strictly speaking, the experimentally determined shape correction factor is not equal to the absolute value of $C(W)$ but rather it is some function that is proportional to $C(W)$, say $C'(W)$ where $C'(W) \propto C(W)$. In order to compare $C'(W)$ with $C(W)$ these quantities must be properly normalized.) The simultaneous theoretical fitting of the shape correction factor and of the beta-gamma angular correlation function yielded limited ranges for the nuclear matrix element parameters effective in the beta transitions of Re^{186} and Re^{188} respectively.

B. Theoretical Formulation

The rank (λ) of the nuclear matrix elements governing a given beta decay must satisfy the following relation:

$$|I_i - I_f| \leq \lambda \leq I_i + I_f \quad (34)$$

where I_i and I_f stand for the initial and final nuclear spins in the beta decay. In the case of first-forbidden beta decay the orbital angular momentum of the leptons is \hbar (neglecting higher orders) and the range

of λ is restricted to $\lambda = 0, 1$ and 2 .

For the $1^- \rightarrow 2^+$ beta transitions in Re^{186} and Re^{188} the following 4 matrix elements can be present (1):

$$\eta u = C_A f i \sigma x r \quad \text{for } \lambda = 1$$

$$\eta x = -C_V f r$$

$$\eta \xi y = -C_V f i \alpha$$

$$\eta z = C_A f B_{ij} \quad \text{for } \lambda = 2$$

$\xi (\equiv \alpha Z / 2\rho)$ is the Coulomb energy factor: ρ is the nuclear radius in units of electron Compton wavelengths, α is the fine structure constant and Z is the atomic number. The nuclear parameters u, x, y and z represent the contributions of the various matrix elements as compared to a standard matrix element η , for which we may choose any nonvanishing matrix element contributing to the beta transition. In the case where $I_i + I_f \geq 2$, it is convenient to take the B_{ij} term as η , i.e.:

$$\eta = | C_A B_{ij} |$$

and thus $z = 1$.

The shape correction factor $C(W)$ and the angular correlation coefficient $A_2(W)$ [$\equiv \epsilon(W)$ in Kotani's (1) notation] in the β - γ angular correlation function:

$$\begin{aligned} W_{\beta-\gamma}(\theta) &= 1 + A_2 P_2(\cos \theta) \\ &= 1 + \epsilon P_2(\cos \theta) \end{aligned} \quad (35)$$

for a $1^- \rightarrow 2^+$ beta transition are complicated functions of the nuclear matrix element parameters.

It is convenient at this point to introduce the following parameter:

$$Y = \xi y - [2/(1 + \gamma_1)] \xi(u + x) \quad (36)$$

where $\gamma_1 = [1 - (\alpha z)^2]^{1/2}$. Then $\epsilon(W)$ and $C(W)$ are given by:

$$\epsilon(W) = (p^2/W)(R_3k + ekW)[C(W)]^{-1} \quad (37)$$

$$C(W) = k[1 + aW + (b/W) + cW^2] \quad (38)$$

where p refers to the beta ray momentum ($p^2 = W^2 - 1$). The parameters R_3k , ek , ak , bk and ck , and hence also the functions $\epsilon(W)$ and $C(W)$ are functions of the nuclear parameters Y , u and x .

C. Method of Analysis

The analysis was performed with the help of an IBM 7040 computer. For a given set of parameters Y , u and x the values of $C(W)$ and $\epsilon(W)$ were calculated, and compared with the experimentally determined values. In order to facilitate the task of determining the nuclear matrix element parameters which fit the experimental data best, the χ^2 value associated with the calculated values of $\epsilon(W)$ was determined. χ^2 is defined as:

$$\chi^2 = \sum_i \left[\frac{[\epsilon_i(\text{calculated}) - \epsilon_i(\text{experimental})]^2}{r_i^2} \right] \quad (39)$$

$$\sum_i (1/r_i)^2$$

where the summations are to be taken over the range of energy values examined in the experiments and where r_i is the experimental error in ϵ_i .

The procedure for the analysis consisted first, in varying the parameters Y , u and x in coarse steps (of order 0.2) and second, in reinvestigating regions of low χ^2 values in smaller steps (of order 0.05). The region of investigation was:

$$-1.50 \leq Y \leq 6.50$$

$$-0.60 \leq u \leq 0.50$$

$$-0.60 \leq x \leq 0.40$$

The minimum value of χ^2 compatible with the experimentally determined shape correction factor $C(W)$ was used as the criterion for determining the nuclear matrix element parameters which fit the experimental data best.

It is noted that the computed and the experimentally determined shape correction factors were normalized to unity at the lowest beta energy, i.e.:

$$CN = C(W)/C(W_{\min.}) \quad (40)$$

where $CN \equiv$ normalized shape correction factor.

D. Re^{186} and Re^{188} Results

In the case of Re^{186} , the range of values for the parameters Y , u and x which fit the experimental data best is given by:

$$Y = 4.45 \pm 0.30$$

$$u = 0.09 \pm 0.05$$

$$x = -0.40 \pm 0.10$$

For a comparison of the experimental results with the theoretically predicted results based on the parameter set:

$$Y = 4.45$$

$$u = 0.09$$

$$x = -0.40$$

for Re^{186} , refer to Table VIII.

In the case of Re^{188} , the range of values for the parameters Y , u and x which fit the experimental data best is given by:

$$Y = 2.74 \pm 0.10$$

$$u = 0.06 \pm 0.02$$

$$x = 0.085 \pm 0.02$$

TABLE VIII

Comparison of Theoretical Predictions Based on the Parameter

Set $Y = 4.45$; $u = 0.09$; $x = -0.40$ with Experimental Results for Re¹⁸⁶.

	W	CN	ϵ
Experimental	1.60	1.000 ± 0.010	0.043 ± 0.004
	1.80	1.000 ± 0.010	0.059 ± 0.004
	2.00	1.000 ± 0.010	0.079 ± 0.004
	2.20	1.000 ± 0.010	0.085 ± 0.004
	2.40	1.000 ± 0.010	0.098 ± 0.004
	2.60	1.000 ± 0.010	0.093 ± 0.006
Theoretical	1.60	1.000	0.046
	1.80	0.999	0.059
	2.00	0.998	0.072
	2.20	0.997	0.084
	2.40	0.997	0.096
	2.60	0.997	0.107

For a comparison of the experimental results with the theoretically predicted results based on the parameter set:

$$Y = 2.74$$

$$u = 0.06$$

$$x = 0.085$$

for Re^{188} , refer to Table IX.

In conclusion, it is noted that the above quoted ranges for the parameters Y, u and x , effective in the beta decays of Re^{186} and Re^{188} respectively, do not necessarily exhaust all permissible solutions. Nonetheless, it is believed that the values obtained for Y, u and x in this investigation represent a valid, albeit possibly not unique, solution for the nuclear matrix element parameters governing the beta transitions in Re^{186} and Re^{188} .

TABLE IX

Comparison of Theoretical Predictions Based on the Parameter
 Set $Y = 2.74$; $u = 0.06$; $x = 0.085$ with Experimental Results for Re^{188} .

	W	CN	ϵ
Experimental	3.01	1.000 ± 0.015	0.133 ± 0.005
	3.22	1.000 ± 0.015	0.151 ± 0.004
	3.42	1.000 ± 0.015	0.161 ± 0.006
	3.61	1.000 ± 0.015	0.176 ± 0.004
	3.81	1.000 ± 0.015	0.183 ± 0.006
	4.01	1.000 ± 0.015	0.201 ± 0.004
	4.21	1.000 ± 0.015	0.216 ± 0.006
Theoretical	3.01	1.000	0.134
	3.22	0.996	0.148
	3.42	0.994	0.161
	3.61	0.994	0.174
	3.81	0.996	0.187
	4.01	0.999	0.200
	4.21	1.005	0.212

CHAPTER IX

CONCLUSION

The experiments described in this thesis strongly suggest that the values of the A_2 coefficients obtained in the decays of Re^{186} and Re^{188} represent the unattenuated directional correlation coefficients. Although the precision of the time spectrum analysis is only 20%, the indications are that no severe attenuation occurs in solid sources, and that the quantity 20% defines an upper limit for the attenuation.

The spectra of the $1^- \rightarrow 2^+$ beta groups in the decays of Re^{186} and Re^{188} have been found to have allowed shapes, in agreement with the recent work of Bashandy (8). For the 935-Kev beta group in Re^{186} , the shape correction factor $C(W)$ is constant within $\pm 1\%$, whereas $C(W)$ for the 1980-Kev beta group in Re^{188} is constant within $\pm 1.5\%$.

A comparison of the accurately determined experimental functions $C(W)$ and $A_2(W)$ with the theoretically predicted functions $C(W)$ and $A_2(W)$ computed for various combinations of the nuclear matrix element parameters permits the determination of the parameter set Y, u and x within a narrower range of values than has been previously possible.

BIBLIOGRAPHY

1. T. Kotani, *Phys. Rev.*, 114, 795 (1959).
2. E. Karlsson, E. Matthias and K. Siegbahn: *Perturbed Angular Correlations*, (North Holland Publishing Co. Amsterdam, 1964).
3. T. B. Novey, M. S. Freedman, F. T. Porter and F. Wagner Jr., *Phys. Rev.*, 103, 942 (1956).
4. H. Dulaney, C. H. Braden, E. T. Patronis and L. D. Wyly, *Phys. Rev.*, 129, 283 (1963).
5. L. D. Wyly, C. H. Braden and H. Dulaney, *Phys. Rev.*, 129, 315 (1963).
6. F. T. Porter, M. S. Freedman, T. B. Novey and F. Wagner Jr., *Phys. Rev.*, 103, 921 (1956).
7. L. Koerts, *Phys. Rev.*, 95, 1358 (1954).
8. E. Bashandy and M. S. El-Nesr, *Nuovo Cimento*, XXIX, No. 5, 1169 (1963).
9. M. W. Johns, C. C. McMullen, I. R. Williams and S. V. Nablo, *Can. J. Phys.*, 34, 69 (1956).
10. K. Siegbahn: *Alpha, Beta and Gamma Ray Spectroscopy*, (North Holland Publishing Co. Amsterdam, 1966), Vol. 2, p. 981.
11. L. C. Biedenharn and M. E. Rose, *Revs. Mod. Phys.*, 25, 729 (1953).
12. A. Abragam and R. V. Pound, *Phys. Rev.*, 92, 943 (1953).
13. G. Goertzel, *Phys. Rev.*, 70, 897 (1946).
14. T. R. Gerholm, R. Othaz and M. S. El-Nesr, *Arkiv For Fysik*, 21, 253 (1962).
15. E. E. Habib, H. Ogata and W. Armstrong, *Can. J. Phys.*, 44, 1157 (1966).
16. R. E. Bell, R. L. Graham and H. E. Petch, *Can. J. Phys.*, 30, 35 (1952).

17. E. E. Habib, University of Windsor, unpublished.
18. H. I. West Jr.: Angular Correlation Correction Factors Via the Method of Rose, UCRL-5451 (1959).
19. K. Siegbahn: Alpha, Beta and Gamma Ray Spectroscopy, (North Holland Publishing Co. Amsterdam, (1966), Vol. 2, p. 1691.
20. Nuclear Data, Vol. 1, No. 2, June 1966.
21. A. McAllindon, M.Sc. Thesis, University of Windsor, 1965.
22. H. Young, M.Sc. Thesis, University of Windsor, 1964.
23. National Bureau of Standards: Tables for the Analysis of Beta Spectra, Appl. Math. Ser. 13, 1952.
24. C. P. Bhalla and M. E. Rose: Table of Electronic Radial Functions at the Nuclear Surface and Tangents of Phase Shifts, ORNL-3207.
25. S. B. Burson and E. B. Shera, Phys. Rev., 136, No. 1B, 1 (1964).

VITA AUCTORIS

The author was born on December 8, 1941 in Windsor, Ontario, where he attended both primary and secondary school. In 1960 he enrolled in the physics program at the University of Windsor and received his B.Sc. in 1963. In 1965 he entered the Graduate School of Physics and subsequently received the degree of M.Sc. in 1965. From 1965 to the present time he has engaged himself in the pursuit of a Ph.D.